LETTER

https://doi.org/10.1038/s41586-018-0253-5

Induction of innate immune memory via microRNA targeting of chromatin remodelling factors

John J. Seeley[1], Rebecca G. Baker[1], Ghait Mohamed[2], Tony Bruns[2,3], Matthew S. Hayden[1,4], Sachin D. Deshmukh[2], Daniel E. Freedberg[5] & Sankar Ghosh[1]*

Prolonged exposure to microbial products such as lipopolysaccharide can induce a form of innate immune memory that blunts subsequent responses to unrelated pathogens, known as lipopolysaccharide tolerance. Sepsis is a dysregulated systemic immune response to disseminated infection that has a high mortality rate. In some patients, sepsis results in a period of immunosuppression (known as 'immunoparalysis')[1] characterized by reduced inflammatory cytokine output[2], increased secondary infection[3] and an increased risk of organ failure and mortality[4]. Lipopolysaccharide tolerance recapitulates several key features of sepsis-associated immunosuppression[5]. Although various epigenetic changes have previously been observed in tolerized macrophages[6–8], the molecular basis of tolerance, immunoparalysis and other forms of innate immune memory has remained unclear. Here we perform a screen for tolerance-associated microRNAs and identify miR-221 and miR-222 as regulators of the functional reprogramming of macrophages during lipopolysaccharide tolerization. Prolonged stimulation with lipopolysaccharide in mice leads to increased expression of miR-221 and mir-222, both of which regulate brahma-related gene 1 (*Brg1*, also known as *Smarca4*). This increased expression causes the transcriptional silencing of a subset of inflammatory genes that depend on chromatin remodelling mediated by SWI/SNF (switch/sucrose non-fermentable) and STAT (signal transducer and activator of transcription), which in turn promotes tolerance. In patients with sepsis, increased expression of miR-221 and miR-222 correlates with immunoparalysis and increased organ damage. Our results show that specific microRNAs can regulate macrophage tolerization and may serve as biomarkers of immunoparalysis and poor prognosis in patients with sepsis.

Lipopolysaccharide (LPS) tolerance is an immunosuppressive form of innate immune memory that can be modelled in vitro by prolonged treatment of bone-marrow-derived macrophages (BMDMs) with LPS (Extended Data Fig. 1a). As a result of this functional reprogramming of macrophages, a majority of LPS-induced genes are transcriptionally silenced (that is, tolerized) and are not expressed upon re-stimulation[7,9] (Extended Data Fig. 1b). Using this in vitro model (Extended Data Fig. 1c–e) we identified microRNAs (miRNAs) with expression patterns that correlate with tolerance (Fig. 1a). We validated these findings using qPCR (Extended Data Fig. 1f, g) and found that several miRNAs are differentially expressed during tolerance but not during an acute LPS response. Levels of miR-222, in particular, increased late during the LPS response (Extended Data Fig. 1g) and correlated with tolerance induction (Fig. 1b). miR-222 was also upregulated to a lesser extent with prolonged stimulation with tumour necrosis factor (TNF) or interleukin-1β (IL-1β) (Extended Data Fig. 1h), which has been shown to weakly induce innate immune tolerance[10,11]. Pre-treatment of BMDMs with interferon gamma (IFNγ), which inhibits LPS tolerance[8], prevented LPS-induced upregulation of miR-222 (Extended Data Fig. 1i). Although miR-221 is processed from the same primary transcript as miR-222[12], mature levels of miR-221 and of miR-222 do not always correlate (Extended Data Fig. 2a–c). Given that miR-221 is not responsive to LPS (Extended Data Fig. 2a) or IFNγ (Extended Data Fig. 2d) in BMDMs, we focused on miR-222 in BMDM experiments.

BMDMs were transfected with an miR-222 mimic and stimulated with LPS to determine whether miR-222 induced reprogramming independently of other tolerogenic factors (Extended Data Fig. 2e). Overexpression of miR-222 inhibited expression of several inflammatory mediators at the protein (Fig. 1c), mRNA (Extended Data Fig. 2f), and primary transcript level (Extended Data Fig. 2g). Conversely, antagonization of miR-222 resulted in increased inflammatory gene expression, even during a naive LPS response. This effect was relatively mild early after stimulation (data not shown), probably owing to low basal levels of miR-222 expression, but increased in magnitude at later time points (Fig. 1d). To test the effect of miR-222 on tolerance, BMDMs were transduced with an miR-222 antagonist and tolerized in vitro. Antagonization of miR-222 reduced the duration and magnitude of suppression of LPS-response genes (Fig. 1e). In some cases, tolerized cells with antagonized miR-222 produced as much IL-6 or IL-12p40 in response to LPS as did non-tolerized cells (Fig. 1f).

In contrast to other genes, *Tnf* was suppressed at the mRNA level but not at the primary transcript level (Extended Data Fig. 2f, g), which suggests that miR-222 regulates *Tnf* through a mechanism that is distinct from that of other tolerized genes. Indeed, the untranslated region (UTR) of *Tnf* has a predicted binding site for miR-222 (Extended Data Fig. 3a). Luciferase reporter assays (Extended Data Fig. 3b) and CRISPR deletions of the predicted binding site (Extended Data Fig. 3c–g) confirmed that *Tnf* is a target of miR-222. However, the post-transcriptional effects of miR-222 on TNF expression do not contribute to the effects of miR-222 on other genes, as shown by the fact that TNF neutralization did not recapitulate the effects of miR-222 overexpression (Extended Data Fig. 3h, i).

Intact *Tnf* transcription suggested miR-222 does not alter Toll-like receptor 4 (TLR4) signalling. Indeed, miR-222 overexpression did not affect LPS-induced IκBα degradation (Extended Data Fig. 4a–c). We therefore filtered computational predictions for miR-222 targets that were expressed in macrophages, did not affect TLR4 signalling and decreased in expression late in the LPS response (between 8 and 24 h of LPS stimulation; Extended Data Table 1). This approach identified *Brg1* as the target most likely to mediate the transcriptional effects of miR-222 during LPS tolerance. BRG1, a catalytic subunit of the SWI/SNF (BAF) complex, evicts polycomb repressive complexes in an ATP-dependent manner, promoting chromatin accessibility and enabling transcription factor recruitment to specific binding sites[13]. Notably, BRG1 is recruited to the promoters of late LPS-response genes, which require SWI/SNF activity for their transcription[14].

The predicted miR-222–*Brg1* binding site is evolutionarily conserved (Extended Data Fig. 4d), and RNA levels of *Brg1* and miR-222 during the LPS response were inversely correlated (Extended Data

[1]Department of Microbiology & Immunology, College of Physicians & Surgeons, Columbia University, New York, NY, USA. [2]The Integrated Research and Treatment Center for Sepsis Control and Care, Jena University Hospital, Jena, Germany. [3]Department of Internal Medicine IV (Gastroenterology, Hepatology, and Infectious Diseases), Jena University Hospital, Jena, Germany. [4]Section of Dermatology, Department of Surgery, Dartmouth-Hitchcock Medical Center, Lebanon, NH, USA. [5]Department of Medicine, Division of Digestive & Liver Disease, College of Physicians & Surgeons, Columbia University, New York, NY, USA. *e-mail: sg2715@columbia.edu

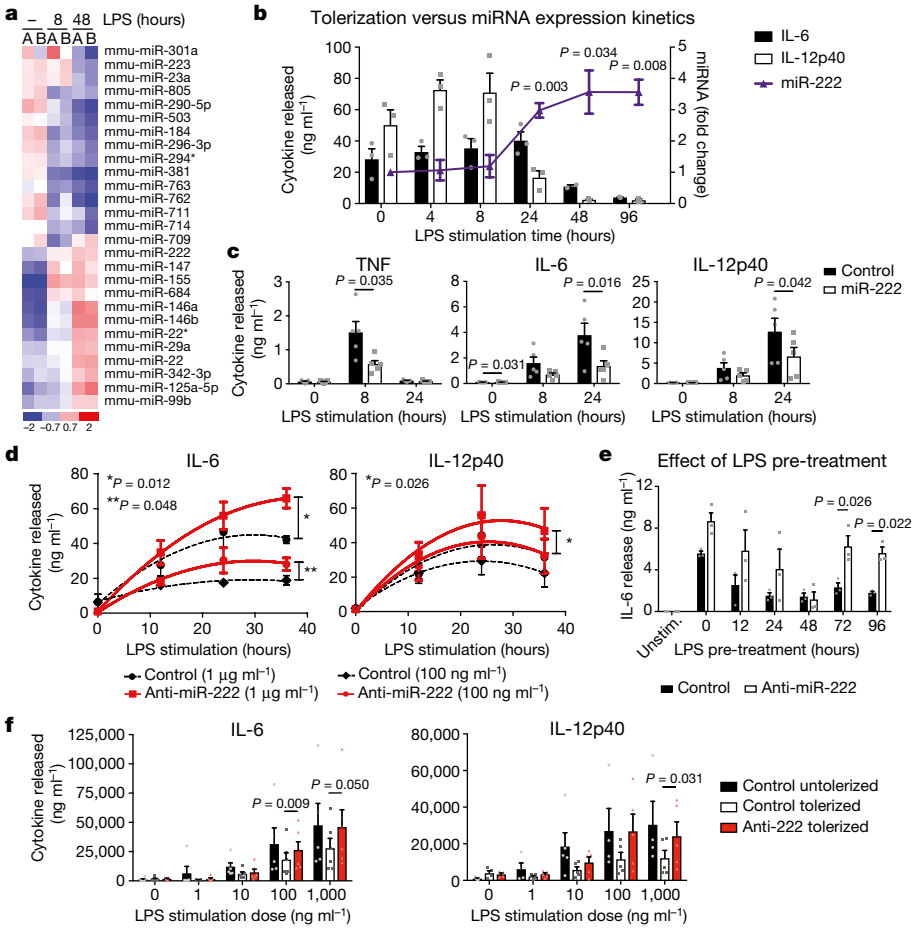

Fig. 1 | miR-222 is upregulated in tolerized BMDMs and suppresses inflammatory gene expression. a, miRNA expression in BMDMs from two mice (labelled A or B) by microarray. **b**, Overlay of qPCR measurement of levels of miR-222 in naive BMDMs (right axis, $n = 4$ biologically independent samples) and cytokine release after re-stimulation of BMDMs as in Extended Data Fig. 1c (left axis, $n = 3$ biologically independent samples) to show the correlation of miR-222 expression kinetics with immunosuppression. **c**, LPS-induced cytokine production after mimic transfection ($n = 5$ biologically independent samples). **d**–**f**, BMDMs (**d**, **f**) or immortalized BMDMs (**e**) were transduced with antagonist constructs. **d**, Cytokine production after stimulation of naive cells ($n = 4$ biologically independent samples). **e**, Re-stimulation of cells with fixed LPS doses after varying pre-treatment time ($n = 3$ independent experiments). **f**, Re-stimulation of cells with varying LPS doses after fixed pre-treatment time ($n = 6$ biologically independent samples). For all graphs, centre value represents mean, and error bars are s.e.m. *P* values calculated by Student's *t*-test (paired, two-sided).

Fig. 4e). Artificial modulation of miR-222 caused an inverse effect on *Brg1* mRNA and protein levels (Extended Data Fig. 4f–h). To confirm that this was due to direct targeting, we cloned the *Brg1* UTR into a luciferase reporter. miR-222 suppressed luciferase activity resulting from co-transfection in a dose-dependent manner only if the miR-222-binding site in the *Brg1* UTR was intact (Extended Data Fig. 4i). We compared the effects of miR-222 overexpression on genes previously identified as being SWI/SNF-dependent in macrophages[15]. Overexpression of miR-222 preferentially suppressed expression of SWI/SNF-dependent genes (Fig. 2a and Extended Data Fig. 4j). Furthermore, BRG1 recruitment to inflammatory gene promoters was reduced after miR-222 overexpression (Fig. 2b). Histone H3 acetylation, which occurs downstream[14] of BRG1 activity, was also reduced (Extended Data Fig. 4k). By contrast, histone H4 acetylation at these promoters, which occurs before BRG1 recruitment[16,17], was unaffected (Extended Data Fig. 4l). Finally, CRISPR–Cas9 disruption of the miR-222-binding site in the *Brg1* UTR in RAW cells (Extended Data Fig. 4m) prevented miR-222-mediated suppression of some SWI/SNF-dependent genes (Extended Data Fig. 4n).

To characterize the biological role of miR-222, we generated a mouse knockout model. However, miR-221 and miR-222 are encoded in the same transcript, are induced by LPS in certain cell types (Extended Data Fig. 2b, c), have similar seed sequences (Extended Data Fig. 5a), have substantial overlap in predicted mRNA targets (Extended Data Fig. 5b) and are both predicted to bind to the same target site in the *Brg1* UTR (Extended Data Fig. 5c). Furthermore, as with miR-222, overexpression of miR-221 downregulates levels of *Brg1* (Extended Data Fig. 5d) and has downstream effects on inflammatory gene expression (Extended Data Fig. 5e). Therefore, we targeted both miRNAs for deletion[18] (Extended Data Fig. 5f–h). We then used qPCR and RNA sequencing to characterize the LPS response in *mir-221 mir-222* knockout macrophages (Fig. 2c). Although the increase in *Brg1* expression in peritoneal macrophages from knockout mice was modest compared to in vitro experiments, *mir-221 mir-222* knockout cells expressed higher levels of many *Brg1*-dependent genes, as well as *Tnf* (Extended Data Fig. 5i, j). Some *Brg1*-dependent genes were more affected by *mir-221 mir-222* knockout than others (compare *Il6* and *Nos2* in Extended Data Fig. 5j), which suggests differential sensitivity to changes in levels of BRG1.

To better understand the mechanisms of altered gene expression in cells that lack miR-221 and miR-222 (Extended Data Fig. 5k), we analysed the promoters of affected genes to identify common regulatory features. Although we obtained similar results in multiple analyses of subsets of affected genes (Extended Data Fig. 6a–f), we limited our main analysis to LPS genes that are most suppressed in tolerized wild-type cells (358 genes out of 1,036 genes in total that are responsive to LPS; Fig. 2d). Roughly half of these 358 genes were expressed at higher levels in tolerized knockout cells compared to tolerized wild-type cells ('de-repressed' genes, Fig. 2e), and roughly half were unaffected

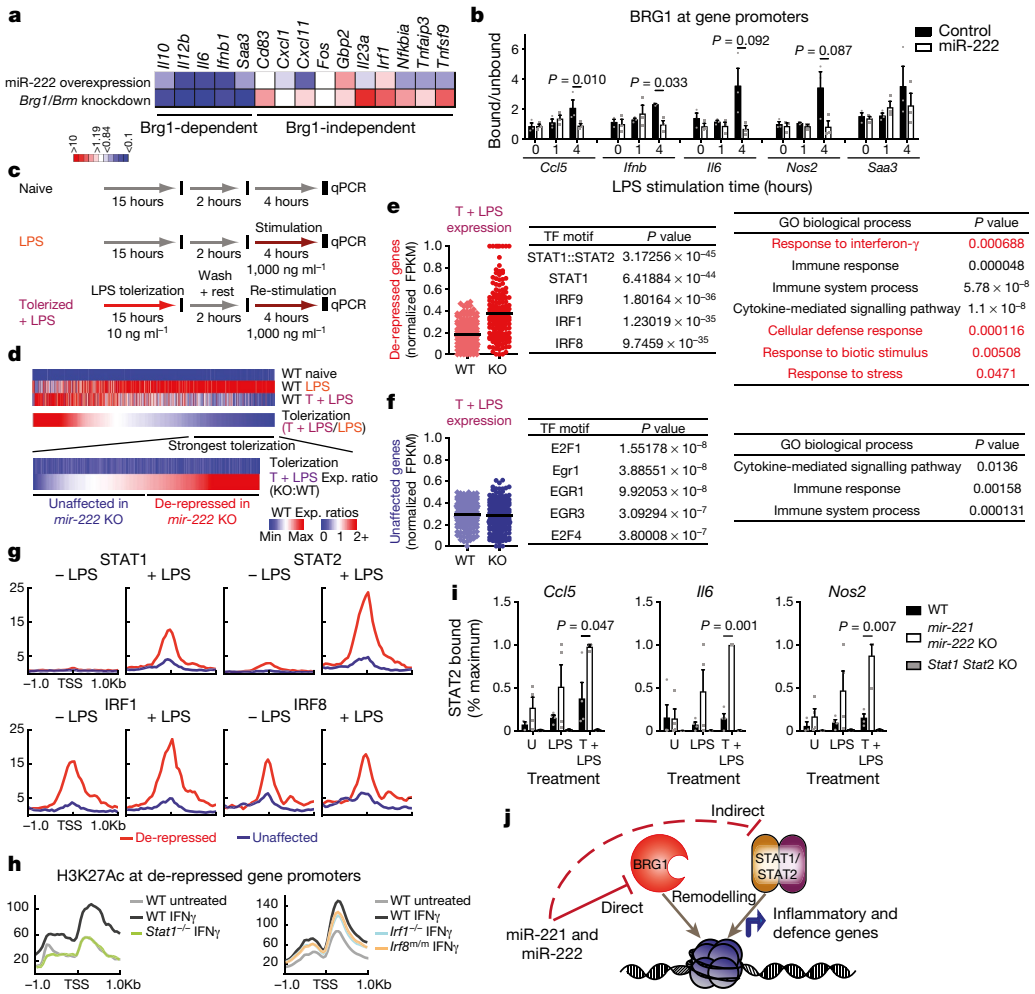

Fig. 2 | miR-222 suppresses BRG1- and STAT-dependent inflammatory gene expression. a, Comparison of miR-222 mimic transfection and the effect of *Brg1* and *Brm* (also known as *Smarca2*) knockdown[15] on LPS-induced gene expression. **b**, ChIP in immortalized BMDMs transduced with overexpression constructs ($n = 3$ independent experiments; P values from Students t-test for paired values, two-sided). **c**, **d**, Schematic of treatments (**c**) and genes (**d**) analysed in **e**–**i**. Exp., expression; KO, knockout; T, tolerized. **e**, **f**, Dot plot of RNA sequencing expression values (normalized to maximal expression per gene) for wild-type (WT) and *mir-221 mir-222* knockout cells (KO), top five predicted[34] transcription factor motifs, and statistically over-represented Gene Ontology (GO) terms (determined by PANTHER) for indicated gene groups ($n = 103$ gene expression values per group). Gene Ontology terms unique to de-repressed genes are highlighted in red. FKPM, fragments per kilobase per million mapped reads; TF, transcription factor. **g**, **h**, Transcription factor occupancy (**g**) and histone modification (**h**) at promoters, quantified from published ChIP–seq datasets[20–25]. *Irf8*$^{m/m}$ is a homozygous mutant with the hypomorphic *Irf8*^{R294C} allele. TSS, transcription start site. **i**, ChIP for STAT2 occupancy in peritoneal macrophages. Values normalized to maximal binding detected for each ChIP (wild type, *mir-221 mir-222* knockout $n = 4$ biologically independent samples; *Stat1 Stat2* knockout, $n = 2$ biologically independent samples. P values were calculated only for wild-type versus *mir-221 mir-222* knockout comparisons, by Student's t-test, two-sided, heteroscedastic). **j**, Model of effect of miR-221 and miR-222 on chromatin at affected gene promoters. For all bar graphs and dot plots, centre represents mean and error bars (if present) represent s.e.m.

('unaffected' genes, Fig. 2f). The promoters of de-repressed genes were enriched for the binding motifs of interferon regulatory factors (IRFs) as well as STAT1 and STAT2 (Fig. 2e), whereas those of unaffected genes were enriched for E2F and EGR family motifs (Fig. 2f). An analysis of predicted downstream functions of the de-repressed gene subset found an enrichment for IFN-response genes (Fig. 2e), and LPS-induced expression of many of these genes is reduced in *Ifnar1* knockout cells[19]. This implies that many of these genes are a part of the late LPS response, transcribed as a result of STAT activation by autocrine and/or paracrine signalling by IFN generated from the initial LPS stimulation.

To determine whether the predicted binding motifs were used during the LPS response, we analysed transcription factor occupancy using previously published chromatin immunoprecipitation followed by sequencing (ChIP–seq) data[20–23]. IRF1 and IRF8 were found to be selectively pre-associated with promoters of de-repressed genes (Fig. 2g and Extended Data Fig. 6g). However, STAT1 and STAT2 were recruited specifically to the promoters of de-repressed genes only after LPS stimulation (Fig. 2g). Other transcription factors, such as NF-κB, were not differentially recruited (Extended Data Fig. 6h). Furthermore, in cells with a deletion or mutation of *Irf1* or *Irf8*, respectively[24], cytokine-induced H3K27 (histone H3, lysine 27) acetylation—a marker of active transcription—was diminished at the promoters of de-repressed genes, whereas deletion of *Stat1*[25] almost completely abolished cytokine-induced H3K27 acetylation at these genes (Fig. 2h). Consistent with this analysis, STAT2 recruitment was significantly higher at the promoters of de-repressed genes in tolerized *mir-221 mir-222* knockout cells after re-stimulation, compared to wild-type cells (Fig. 2i). Furthermore, levels of *Stat1* mRNA are higher in *mir-221 mir-222* knockout cells and in cells in which *Brg1* is overexpressed (Extended Data Fig. 7i, j) than they are in wild-type cells. Therefore, miR-221 and miR-222 perturb SWI/SNF promoter recruitment, which leads to the repression of STAT activity at inflammatory gene promoters. As BRG1 and STAT transcription factors work cooperatively only at certain gene promoters to enable IFN- and cytokine-induced gene transcription[26,27], miR-221 and miR-222 may limit expression of specific genes (Fig. 2i).

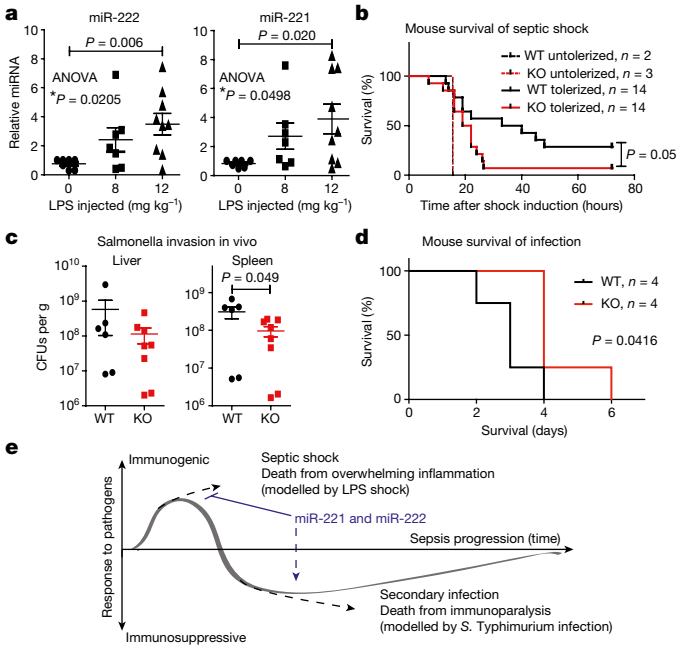

Fig. 3 | miR-221 and miR-222 protect against inflammatory septic shock but increase susceptibility to live infection in mice. a, miRNA levels in blood buffy coat 24 h after LPS injection ($n = 7$ mice for dose 0, 7 mice for dose 8 mg per kg and 9 mice for dose 12 mg per kg). **b**, Survival of littermates that were untreated or tolerized before lethal LPS injection, as in Extended Data Fig.. **c**, **d**, Bacterial dissemination (**c**, $n = 6$ wild-type and 8 knockout mice) and host survival (**d**) after intraperitoneal injection with *S.* Typhimurium. **e**, Model of miR-221 and miR-222 effect on the immune response and host survival during the course of sepsis. For **a**, **c**, *P* values were determined by Student's *t*-test (paired, two-sided). *P* values for **b**, **d**, log-rank (Mantel–Cox) test (performed only for $n > 3$). For all dot plots, centre line represents mean; error bars represent s.e.m.

Next, we examined miR-221 and miR-222 activity using a model of sterile inflammatory shock induced by a high-dose LPS injection. In this system, changes that decrease inflammation increase survival: therefore, we used this model mainly to determine whether the anti-inflammatory effects of miR-221 and miR-222 we observe in vitro also occur in vivo. After LPS injection, levels of miR-221 and miR-222 in circulating immune cells were elevated (Fig. 3a). To determine whether this is physiologically relevant, LPS tolerance was induced in wild-type and *mir-221 mir-222* knockout littermates by administering two sublethal doses of LPS before a lethal LPS dose: this regimen induces sufficient tolerance to prevent lethality in wild-type mice (Extended Data Fig. 7a, b). Although *mir-221 mir-222* knockout mice were also protected from lethality, the *mir-221 mir-222* knockout mice exhibited more symptoms of septic shock (Extended Data Fig. 7c), which indicates decreased anti-inflammatory effects in the knockouts. To test whether miR-221 and miR-222 contribute to survival under more extreme conditions, we used a model of septic shock in which tolerance is only partially protective against lethality (Extended Data Fig. 7d, e). In this model, absence of miR-221 and miR-222 decreased the median survival time (from 36.5 h to 20.5 h) as well as the likelihood of septic shock survival over a 72-h period (Fig. 3b).

Although LPS-induced septic shock is used to study acute inflammation in vivo, this model does not recapitulate sepsis in patients or necessarily predict the effect of inflammatory regulators on patient outcome. Therefore, to study the role of miR-221 and miR-222 in a model that better reflects the systemic innate response to pathogen challenge, we used a *Salmonella enterica* subsp. *enterica* serovar Typhimurium (*S.* Typhimurium) infection model. First, we performed in vitro assays using green fluorescent protein (GFP)-expressing *S.* Typhimurium to infect BMDMs. BMDMs from *mir-221 mir-222* knockout mice exhibited increased GFP per cell soon after infection (Extended Data Fig. 7f–h). At later time points, this difference was not observed (Extended Data Fig. 7h), which suggests that—despite increased phagocytosis—*mir-221 mir-222* knockout cells are more efficient at suppressing intracellular replication and/or survival. We confirmed this finding by lysing BMDMs and comparing bacterial colony-forming unit (CFU) recovery at early and late time points after infection (Extended Data Fig. 7i). To test miR-221 and miR-222 effects in vivo, wild-type and knockout mice were injected intraperitoneally with the same strain of *S.* Typhimurium. Two days after infection, fewer bacterial CFUs were recovered from the liver and spleen of *mir-221 mir-222* knockout mice (Fig. 3c). In addition, *mir-221 mir-222* knockout mice exhibited increased survival time (Fig. 3d), suggesting that the loss of miR-221 and miR-222 confers resistance to bacterial replication and/or dissemination. These findings suggest that miR-221 and miR-222 broadly suppress inflammation and innate immune function. During the early stages of sepsis expression of miR-221 and miR-222 may be protective, by limiting the excessive inflammatory cytokine production that contributes to septic shock. Conversely, miR-221 and miR-222 appear to contribute to immunoparalysis, and increased miR-221 and miR-222 expression may enhance lethality during the later stages of sepsis (Fig. 3e).

Because it is unclear which models most accurately resemble conditions in patients, we next examined miR-221 and miR-222 expression in human disease. Consistent with results from mouse cells, miR-221 and miR-222 are both upregulated in response to prolonged LPS stimulation of a human monocyte-like cell line, whereas only miR-222 is upregulated by LPS in this cell line after phorbol 12-myristate 13-acetate (PMA)-induced differentiation to a macrophage-like cell type (Extended Data Fig. 8a, b). Next we analysed miR-221 and miR-222 expression in three patient cohorts. In the first cohort (Extended Data Fig. 8c), we quantified miR-221 and miR-222 levels in peripheral blood mononuclear cells from ten sequential patients from an intensive care unit, who met sepsis criteria[28] within 4 h of admission to the intensive care unit. Compared to peripheral blood mononuclear cells from healthy donors, miR-221 and miR-222—but not several other inflammation-associated miRNAs—were significantly higher in samples from patients in the intensive care unit (Fig. 4a). Levels of miR-221 and miR-222 expression were then examined in a second cohort of patients, all of whom had acute decompensated liver disease and clinical suspicion of infection (Extended Data Fig. 8d). Patients with organ failure, as defined by the chronic liver failure–sequential organ failure assessment, had significantly higher levels of miR-222 than patients without such failure (Fig. 4b). Levels of miR-221 correlated with those of miR-222 (Extended Data Fig. 8f), but were not increased to statistically significant levels (Fig. 4c). Levels of miR-222 in this cohort inversely correlated with levels of *BRG1* expression (Fig. 4d). In a set of matched peripheral blood mononuclear cell and serum samples, levels of miR-222 and TNF were also inversely correlated (Fig. 4e). Finally, the inverse correlation between miR-222 and *BRG1* was also observed in $CD14^+$ monocytes sorted from the peripheral blood mononuclear cell population of a third clinical cohort (Fig. 4f and Extended Data Fig. 8e), confirming changes in levels of miR-222 and *BRG1* in myeloid cells.

Unlike generalized inflammatory markers, miR-222 elevation correlates specifically with severe sepsis. miR-222 levels do not correlate with inflammatory markers such as C-reactive protein or white blood cell count, but showed a significant correlation with organ-damage markers, including creatinine and the model for end-stage liver disease score (Extended Data Fig. 8g–j). miR-222 expression may be a useful biomarker for detecting patients who are undergoing septicaemia-induced immunoparalysis and are, therefore, predisposed to organ failure and mortality.

In summary, our data establish a model in which miR-221 and miR-222 restrict chromatin remodelling and silence transcription to enforce innate immune tolerance. After prolonged innate immune signalling, increased expression of miR-221 and miR-222 reduces expression of BRG1, which leads to changes in SWI/SNF complex levels or composition that result in the selective expression of only those LPS-response genes with the most favourable chromatin states. The fact that substantial changes in gene expression result from modest miR-221- and miR-222-dependent

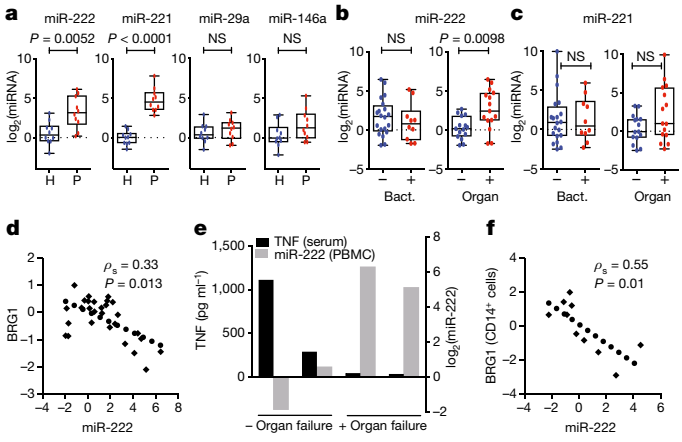

Fig. 4 | miR-222 correlates with immunosuppression and severe sepsis in patients. a, miRNA expression in peripheral blood mononuclear cells from healthy donors (H) or patients (P) from the intensive care unit with sepsis ($n = 10$ per group). *P* values, two-sided Mann–Whitney *U* test. **b**, **c**, Expression in peripheral blood mononuclear cells from a cohort of patients with chronic liver disease, stratified for bacterial infection ($n = 20$ patients negative (−), 10 positive (+)) and inflammation-related organ failure (acute-on-chronic liver failure; $n = 15$ patients per group). *P* values, two-sided Mann–Whitney *U* test. Bact., cells from patients with bacterial infection; organ, cells from patients with organ failure. **d**, **f**, Correlation of RNA levels in peripheral blood mononuclear cells (**d**, $n = 28$ patients) or $CD14^+$ monocytes of patients with multiple organ failure (**f**, $n = 10$ patients). Spearman's rho (ρ) and *P* values from bivariate non-parametric regression analysis. **e**, Correlation of serum TNF and miR-222 expression in peripheral blood mononuclear cells (PBMC) from four patients with signs of infection. Two patients had organ failure according to the EASL CLIF-C criteria for acute-on-chronic liver failure. In box and whisker plots, median is shown as centre line; box, 25th to 75th percentiles; whiskers, minimum to maximum values. NS, not significant.

changes in BRG1 expression is consistent with previous reports that the mutation or deletion of a single allele of the SWI/SNF subunit is sufficient to confer strong phenotypic effects[29,30]. Hence, by fine-tuning the levels of BRG1, miR-221 and miR-222 can prevent prolonged expression of STAT-dependent inflammatory genes in macrophages, thereby leading to tolerance or innate immunoparalysis (Extended Data Fig. 9). By contrast, robust activation of STAT1—for example, by co-stimulation with IFNγ—can block[8] or even reverse[31,32] LPS tolerance and innate immunoparalysis. Consistent with such a role for STAT1, treatment with IFNγ has been shown to improve outcomes in sepsis[33].

Although LPS tolerance promotes survival in mouse models of sterile shock, patients with sepsis probably succumb to primary or secondary[1] infections owing to immunosuppression as a result of functional reprogramming of myeloid cells. Thus, the same innate immunoparalysis that is protective in the mouse LPS-shock model would be responsible for organ damage and mortality in human patients with sepsis. We identify miR-221 and miR-222 as mediators of tolerance and show that miR-221 and miR-222 expression may distinguish patients with organ failure who are at high risk of mortality from those patients with infection alone. Thus, the monitoring of miR-221 and miR-222, or related bio-markers, may help clinicians to stratify patients with sepsis into groups on the basis of whether they would benefit from pro-inflammatory immunotherapies or classical anti-inflammatory treatments.

Online content

Any Methods, including any statements of data availability and Nature Research reporting summaries, along with any additional references and Source Data files, are available in the online version of the paper at https://doi.org/10.1038/s41586-018-0253-5.

Received: 28 February 2017; Accepted: 3 May 2018;
Published online 27 June 2018.

1. Hotchkiss, R. S., Monneret, G. & Payen, D. Sepsis-induced immunosuppression: from cellular dysfunctions to immunotherapy. *Nat. Rev. Immunol.* **13**, 862–874 (2013).
2. Ertel, W. et al. Downregulation of proinflammatory cytokine release in whole blood from septic patients. *Blood* **85**, 1341–1347 (1995).
3. Otto, G. P. et al. The late phase of sepsis is characterized by an increased microbiological burden and death rate. *Crit. Care* **15**, R183 (2011).
4. Boomer, J. S. et al. Immunosuppression in patients who die of sepsis and multiple organ failure. *J. Am. Med. Assoc.* **306**, 2594–2605 (2011).
5. Cavaillon, J. M. & Adib-Conquy, M. Bench-to-bedside review: endotoxin tolerance as a model of leukocyte reprogramming in sepsis. *Crit. Care* **10**, 233 (2006).
6. Saeed, S. et al. Epigenetic programming of monocyte-to-macrophage differentiation and trained innate immunity. *Science* **345**, 1251086 (2014).
7. Foster, S. L., Hargreaves, D. C. & Medzhitov, R. Gene-specific control of inflammation by TLR-induced chromatin modifications. *Nature* **447**, 972–978 (2007).
8. Chen, J. & Ivashkiv, L. B. IFN-γ abrogates endotoxin tolerance by facilitating Toll-like receptor-induced chromatin remodeling. *Proc. Natl Acad. Sci. USA* **107**, 19438–19443 (2010).
9. Mages, J., Dietrich, H. & Lang, R. A genome-wide analysis of LPS tolerance in macrophages. *Immunobiology* **212**, 723–737 (2008).
10. Fraker, D. L., Stovroff, M. C., Merino, M. J. & Norton, J. A. Tolerance to tumor necrosis factor in rats and the relationship to endotoxin tolerance and toxicity. *J. Exp. Med.* **168**, 95–105 (1988).
11. Cavaillon, J.-M., Pitton, C. & Fitting, C. Endotoxin tolerance is not a LPS-specific phenomenon: partial mimicry with IL-1, IL-10 and TGFβ. *J. Endotoxin Res.* **1**, 21–29 (1994).
12. Di Leva, G. et al. MicroRNA cluster 221–222 and estrogen receptor α interactions in breast cancer. *J. Natl. Cancer Inst.* **102**, 706–721 (2010).
13. Stanton, B. Z. et al. *Smarca4* ATPase mutations disrupt direct eviction of PRC1 from chromatin. *Nat. Genet.* **49**, 282–288 (2017).
14. Ramirez-Carrozzi, V. R. et al. Selective and antagonistic functions of SWI/SNF and Mi-2β nucleosome remodeling complexes during an inflammatory response. *Genes Dev.* **20**, 282–296 (2006).
15. Ramirez-Carrozzi, V. R. et al. A unifying model for the selective regulation of inducible transcription by CpG islands and nucleosome remodeling. *Cell* **138**, 114–128 (2009).
16. Saccani, S., Pantano, S. & Natoli, G. Two waves of nuclear factor κB recruitment to target promoters. *J. Exp. Med.* **193**, 1351–1359 (2001).
17. Agalioti, T., Chen, G. & Thanos, D. Deciphering the transcriptional histone acetylation code for a human gene. *Cell* **111**, 381–392 (2002).
18. Park, C. Y. *et al.* A resource for the conditional ablation of microRNAs in the mouse. *Cell Reports* **1**, 385–391 (2012).
19. Ourthiague, D. R. et al. Limited specificity of IRF3 and ISGF3 in the transcriptional innate-immune response to double-stranded RNA. *J. Leukoc. Biol.* **98**, 119–128 (2015).
20. Mancino, A. et al. A dual *cis*-regulatory code links IRF8 to constitutive and inducible gene expression in macrophages. *Genes Dev.* **29**, 394–408 (2015).
21. Tong, A. J. et al. A stringent systems approach uncovers gene-specific mechanisms regulating inflammation. *Cell* **165**, 165–179 (2016).
22. Garber, M. et al. A high-throughput chromatin immunoprecipitation approach reveals principles of dynamic gene regulation in mammals. *Mol. Cell* **47**, 810–822 (2012).
23. Cohen, M. et al. Chronic exposure to TGFβ1 regulates myeloid cell inflammatory response in an IRF7-dependent manner. *EMBO J.* **33**, 2906–2921 (2014).
24. Langlais, D., Barreiro, L. B. & Gros, P. The macrophage IRF8/IRF1 regulome is required for protection against infections and is associated with chronic inflammation. *J. Exp. Med.* **213**, 585–603 (2016).
25. Ostuni, R. et al. Latent enhancers activated by stimulation in differentiated cells. *Cell* **152**, 157–171 (2013).
26. Huang, M. et al. Chromatin-remodelling factor BRG1 selectively activates a subset of interferon-α-inducible genes. *Nat. Cell Biol.* **4**, 774–781 (2002).
27. Ni, Z. et al. Apical role for BRG1 in cytokine-induced promoter assembly. *Proc. Natl Acad. Sci. USA* **102**, 14611–14616 (2005).
28. Levy, M. M. et al. 2001 SCCM/ESICM/ACCP/ATS/SIS International Sepsis Definitions Conference. *Intensive Care Med.* **29**, 530–538 (2003).
29. Kadoch, C. et al. Proteomic and bioinformatic analysis of mammalian SWI/SNF complexes identifies extensive roles in human malignancy. *Nat. Genet.* **45**, 592–601 (2013).
30. Bultman, S. et al. A *Brg1* null mutation in the mouse reveals functional differences among mammalian SWI/SNF complexes. *Mol. Cell* **6**, 1287–1295 (2000).
31. Cheng, S. C. et al. Broad defects in the energy metabolism of leukocytes underlie immunoparalysis in sepsis. *Nat. Immunol.* **17**, 406–413 (2016).
32. Leentjens, J. et al. Reversal of immunoparalysis in humans *in vivo*: a double-blind, placebo-controlled, randomized pilot study. *Am. J. Respir. Crit. Care Med.* **186**, 838–845 (2012).
33. Döcke, W. D. et al. Monocyte deactivation in septic patients: restoration by IFN-γ treatment. *Nat. Med.* **3**, 678–681 (1997).
34. Zambelli, F., Pesole, G. & Pavesi, G. Pscan: finding over-represented transcription factor binding site motifs in sequences from co-regulated or co-expressed genes. *Nucleic Acids Res.* **37**, W247–W252 (2009).

Acknowledgements We thank M. McManus (UCSF) for generously providing us with a targeting construct used in the generation of *mir-221 mir-222* knockout

mice. This work was supported by grants R21-AI116082 and R37-AI33443 to S.G. from the National Institutes of Health.

Reviewer information *Nature* thanks G. Crabtree, R.Hotchkiss, M. Netea and the other anonymous reviewer(s) for their contribution to the peer review of this work.

Author contributions J.J.S. performed the majority of the experiments and writing of the manuscript. R.G.B. performed the microRNA microarray experiment. G.M. performed experiments on patient samples. T.B., S.D.D. and D.E.F. assisted with experimental design and collected patient samples for the human portions of this study. M.S.H. assisted with experimental design and the writing of the manuscript. S.G. conceived the study, and provided guidance with experimental design and the writing of the manuscript.

Competing interests The authors declare no competing interests.

Additional information
Extended data is available for this paper at https://doi.org/10.1038/s41586-018-0253-5.
Supplementary information is available for this paper at https://doi.org/10.1038/s41586-018-0253-5.
Reprints and permissions information is available at http://www.nature.com/reprints.
Correspondence and requests for materials should be addressed to S.G.
Publisher's note: Springer Nature remains neutral with regard to jurisdictional claims in published maps and institutional affiliations.

METHODS

Cell culture. RAW 264.7 cells (ATCC TIB-7) were cultured in DMEM supplemented with 10% fetal bovine serum. 293FT cells (Invitrogen R7007) and L-929 cells (ATCC CCL-1) were cultured in DMEM supplemented with 10% fetal bovine serum. Cells were purchased from vendor and tested for mycoplasma contamination before use (no further authentication of line identity was performed). L-cell conditioned medium (LCM) was generated by filter-sterilizing the supernatant of L-929 cells that were allowed to grow for one week in culture. Primary BMDMs were generated by isolation and culture of mouse bone marrow in complete RPMI supplemented with 20% LCM for up to 12 days. Immortalization of BMDMs was performed as previously described[35] by inoculation with the J2 retrovirus. For cell stimulations, 10 ng/ml LPS (Sigma L8274), 10 ng/ml recombinant human TNF (R&D Systems 210-TA), 100 ng/ml recombinant mouse IL-1β (R&D Systems 401-ML-005), 100 ng/ml recombinant mouse IFNγ (BD Pharmingen 554587), 10 pg/ml recombinant mouse IL-10 (eBioScience 88-7104-ST), 10 μM dexamethasone (Sigma D402) and 0.01 μM oestrogen (Sigma E2758) were used unless otherwise indicated. For tolerization experiments, BMDMs were stimulated with 10 ng/ml LPS for 15 h (or as indicated), washed 5 times with 1× PBS, then allowed to rest for 2 h in LPS-free complete medium supplemented with 20% LCM. BMDMs were then stimulated with 1 μg/ml LPS for 4 h (for qPCR) or 12 h (for enzyme-linked immunosorbent assay (ELISA)), or as indicated.

miRNA microarray. Samples were treated as described, rinsed with 1× PBS, lysed in TRIzol and sent to a commercial microRNA array profiling service (Exiqon). As part of the service, samples were labelled using the miRCURY Hy3/Hy5 Power labelling kit and hybridized on the miRCURY LNA array (v.11.0 hsa, mmu and rno). All capture probes for the control spike-in oligonucleotides produced signals in the expected range. The quantified background-corrected signals were normalized using the global Lowess (locally weighted scatterplot smoothing) regression algorithm, and a list of differentially expressed miRNAs was returned.

miRNA mimic and antagonist oligonucleotides. Pre-miR miRNA precursors (Ambion AM17100) and anti-miR miRNA inhibitors (Ambion AM17000) were transfected into BMDMs to modulate miRNA function in short-term experiments. Part numbers for oligonucleotides are as follows: for overexpression experiments, pre-miR negative control #1 (Invitrogen AM17110), miR-222-3p (PM11376), miR-221-3p (PM10337); for antagonization experiments, anti-miR miRNA negative control #1 (Ambion AM17010), miR-222-3p (AM11376), miR-221-3p (AM10337). To optimize transfection conditions, the FAM dye-labelled pre-miR negative control #1 (Invitrogen AM17121) oligonucleotide was used. Transfection of 50,000 BMDMs per well of a 12-well plate with 6 μl lipofectamine and 0.1 nmol oligonucleotide diluted in 200 μl of Opti-MEM (total) was found to provide transfection of >80% of cells (as measured by flow cytometry), and these conditions were used for all further experiments in BMDMs. Medium was replaced with complete RPMI containing 20% LCM after 4 h to minimize cytotoxicity. Cells were allowed to recover for 24–48 h before stimulation.

Production of virus and BMDM transduction. Plasmids for miRNA overexpression (GeneCopoeia CmiR0001-MR01, MmiR3289-MR01, or MmiR3434-MR01) or antagonization (GeneCopoeia CmiR-AN0001-a.m.03 or HmiR-AN0399-a.m.03) were transfected into 293FT cells with the Lenti-Pac HIV Expression Packaging Kit (GeneCopoeia HPK-LVTR-20) or Lenti-Pac FIV Expression Packaging Kit (GeneCopoeia FPK-LVTR-20) to generate viral particles. BMDMs were inoculated by spin infection in 6-well plates in the presence of 6 μg/ml polybrene (Sigma H9268). Following spin inoculation, viral supernatant was immediately replaced with complete RPMI supplemented with 20% LCM. Cells were allowed to recover overnight. For primary BMDMs, plating for inoculation was generally performed on day five of differentiation. The first spin infection was performed on day six, second spin infection (if necessary) was performed on day seven, and plating for experiments was performed on day eight.

ELISA. BMDMs were plated at 50,000 cells per well, and cytokine concentrations in cell supernatants were measured using the BD OptEIA Mouse IL-6 ELISA Set (BD 555240), BD OptEIA Mouse IL-12 (p40) ELISA Set (BD 555165), or BD OptEIA Mouse TNF (Mono/Mono) ELISA Set (BD 555268) according to the manufacturer's instructions.

RNA extraction, reverse transcription and qPCR. Total RNA was extracted from samples using TRIzol reagent (Invitrogen 15596018). For reverse transcription and detection of miRNAs, the Universal cDNA Synthesis Kit (Exiqon 203301) and locked nucleic acid primers (Exiqon) were used. For other genes, approximately 1 μg of RNA was reverse transcribed with SuperScript III (Invitrogen 18080085). qPCR was then performed with VeriQuest Fast SYBR (Affymetrix 75675). The amplified transcripts were quantified using the comparative C_t method.

Computational prediction of miRNA-binding sites. miR-222-binding sites were predicted using the PITA algorithm[36] (http://genie.weizmann.ac.il/pubs/mir07/mir07_prediction.html) or MicroCosm Targets program (which utilizes the miRanda algorithm) as indicated in the text. MicroCosm Targets Version 5 was used to search for targets for mmu-miR-222[37]. UTRs and miRNA sequences were manually input to the PITA algorithm, and default search settings were used. All predictions were re-verified with their respective programs on 5 December 2013.

Construction of reporter vectors and luciferase reporter assays. The *Brg1* UTR was amplified from IMAGE clone 30533489 (Open Biosystems MMM1013-9498346) and cloned into the pMIR-Report (Ambion AM5795) multiple cloning site using HindIII and SpeI restriction sites. The *Tnf* UTR was amplified from cDNA generated from BMDMs stimulated with LPS for 1 h, and inserted into the pMIR-Report vector as performed for the *Brg1* UTR. Reporter plasmids were transfected into 293FT cells along with a Renilla luciferase reporter (used to normalize for transfection efficiency). After 24 h, Firefly and Renilla luciferase activity was quantified using the Dual-Luciferase Reporter Assay (Promega E1980).

CRISPR. The CRISPR design tool (http://crispr.mit.edu) was used to design guide RNAs for cloning into the PX458 (Addgene 48138) and PX459 (Addgene 48139) dual Cas9 and single-guide RNA expression plasmids[38] to generate plasmids to target identified miR-222-binding sites for deletion. Cells were transiently transfected with empty vector or targeting vectors. After 24 h, transfected cells were selected using 48 h of puromycin treatment (PX459) or by sorting for GFP positive (PX458) cells. Limiting dilution was performed to isolate clonal cell lines. Clones were screened for appropriate deletion by PCR. Deletion of targeted regions was confirmed by sequencing when necessary. Gene expression was compared between lines with successful deletion, unsuccessful deletion and lines generated by transfection with expression plasmids that lacked a Cas9-targeting sequence.

For deletion of the miR-222-binding site in the *Tnf* UTR, the following guide sequences were used: combination 1, TCAGCGTTATTAAGACAATT GGG and ATTACAGTCACGGCTCCCGT GGG; combination 2, TTGTCTTAATAACGCTGATT TGG and ATTTCTCTCAATGACCCGTA GGG. For deletion of the miR-222-binding site in the *Brg1* UTR, the following guide sequences were used: GGAGTAGCCCTTAGCAGTGA TGG and ACCAGATGTAGTTTCGAACT TGG.

Intracellular staining for flow cytometry. Cells were rinsed and fixed for 15–30 min at room temperature in 4% paraformaldehyde. Cells were rinsed and permeabilized by resuspension in 5% saponin for 10–20 min at room temperature. Either anti-IκBα (L35A5, Cell Signaling 4814), anti-Brg1 (H88, Santa Cruz sc-10768), or rabbit monoclonal antibody IgG isotype control (Cell Signaling 3900) was added, and cells were incubated for an additional 20 min at room temperature. Cells were rinsed and re-suspended in saponin with 1:300 dilution of fluorochrome-conjugated secondary antibody (Alexa Fluor 488 donkey anti-rabbit IgG, Invitrogen A21206; Alexa Fluor 546 goat anti-rabbit IgG, Invitrogen A11010; or Alexa Fluor 546 donkey anti-mouse IgG, Invitrogen A10036). After incubation at room temperature for 20 min, cells were rinsed, re-suspended in PBS and analysed on a BD LSRII flow cytometer.

Chromatin immunoprecipitation. Cells from a 15-cm plate were fixed by incubation in 1% formaldehyde for 5 min, rinsed and lysed by incubation for 5 min on ice in buffer L1 (50 mM Tris at pH 9, 2 mM EDTA, 0.1% NP-40, 10% glycerol, with protease inhibitors). Nuclei were spun down and re-suspended in 500 μl buffer L2 (50 mM Tris at pH 8, 0.1% sodium dodecyl sulphate and 5 mM EDTA). Sonication was performed in a Bioruptor, using 10 cycles of 30 s each. Immunoprecipitation was performed using 20 μl magnetic protein A beads and 5 μg anti-acetyl-histone H4 (Lys5; Millipore 07-327), 2 μg anti-BRG1 (H-88; Santa Cruz sc-10768), or 5 μg anti-acetyl-histone H3 (Millipore 06-599) per 50 μl of chromatin in a 500 μl volume. After overnight rotation at 4 °C, supernatant was isolated. DNA was recovered from the supernatant by adding 20 μl of 5 M NaCl, 50 μl of 10% SDS and 5 μl of proteinase K, shaking for 2 h at 60 °C (unbound fraction). Beads were washed 3× in high salt buffer (20 mM Tris at pH 8.0, 0.1% SDS, 1% NP-40, 2 mM EDTA, and 0.5 M NaCl), and 3× in Tris–EDTA. DNA was eluted from beads by re-suspending beads in 100 μl elution buffer and shaking for 2 h at 60 °C (bound fraction). Bound and unbound fractions were heated to 95 °C for 10 min. DNA was purified from fractions using the Qiagen PCR Purification Kit (28104). To check for promoter binding, qPCR was performed using DNA from the bound and unbound fractions. Bound:unbound ratios were normalized to alpha-crystallin ratios, as this should represent a silent gene.

Amaxa nucleofection. BMDMs were nucleofected with 2 μg of plasmid DNA using the Amaxa Mouse Macrophage Nucleofector Kit (VPA-1009), in conjunction with the Amaxa Nucleofector II Device, according to the manufacturer-optimized protocol.

***Salmonella enterica* serovar Typhimurium infection.** For these experiments, a GFP-expressing *Salmonella enterica* serovar Typhimurium strain (SL1344) was used. *S.* Typhimurium cultures were grown in LB medium supplemented with 100 μg/ml carbenicillin and 30 μg/ml streptomycin. Overnight cultures were diluted and allowed to grow for an additional hour before use, to ensure bacteria were in log-growth phase. $OD_{600\,nm}$ readings were correlated to previously determined CFU values and used to quantify number of bacteria present in culture. BMDMs were infected by inoculation of DMEM growth medium (containing only streptomycin) with bacteria at a multiplicity of infection of 50. Plates were spun at 800 r.c.f. for

5 min at 4 °C. BMDMs were incubated for 30 min at 37 °C. Cells were washed 3 times, and then incubated in medium containing gentamycin (100 μg/ml for incubations of 2 h or less, 12 μg/ml for longer incubations). BMDMs were subsequently analysed for GFP content by flow cytometry, or lysed in water to enable plating of lysate dilutions on LB agar plates containing carbenicillin to determine bacterial CFU counts.

Mice. For BMDM generation, female C57Bl/6J mice of 7–10 weeks of age were used, unless otherwise noted. For tolerance and septic shock experiments, male C57Bl/6J mice of 6–10 weeks of age were used. LPS (*Escherichia coli* O55:B5; Sigma L2880) and D-(+)-galactosamine hydrochloride (Sigma G0500) were re-suspended in sterile PBS and filter-sterilized before intraperitoneal injection. For in vivo infection experiments, mice were given intraperitoneal injections of 1×10^7 CFUs per kg of a GFP-expressing *Salmonella enterica* serovar Typhimurium strain (SL1344) suspended in PBS. Mice were maintained under specific-pathogen-free conditions in animal facilities at Columbia University Medical Center. All animal experiments were carried out with the approval of the Columbia University Institutional Animal Care and Use Committee, and in compliance with regulations and guidelines set forth by Columbia University.

Generation of knockout mice. *mir-221 mir-222* knockout mice were generated at the Columbia University Transgenic Mouse facility. In brief, KV1 (129B6 hybrid) ES cells were electroporated with the linearized targeting construct discussed in Extended Data Fig. 6. After positive and negative selection, clonal cell lines were screened by PCR for proper integration of the construct. Positive lines were expanded, blastocyst injection was performed and germline transmission was confirmed. *mir-221 mir-222* knockout mice were backcrossed to the C57Bl/6 background 5–8 times before experimental use.

Peritoneal macrophage isolation. Five millilitres of cold PBS was injected into the peritoneal cavity of euthanized mice. The peritoneum was gently massaged. Fluid was collected and the process was repeated. Cell suspension was spun down and cells were plated at 500,000 cells per well in 12-well plates. Macrophages were allowed to adhere overnight. Non-adherent cells were rinsed off with PBS washes.

Thioglycollate elicitation of peritoneal macrophages. Three per cent thioglycollate was sterilized and aged for at least two months. One millilitre of thioglycolate preparation was injected into the peritoneal cavity of each mouse five days before the isolation of macrophages (as described in 'Peritoneal macrophage isolation').

Monocyte isolation. Bones were isolated from wild-type C57Bl6/J mice. Marrow was retrieved by crushing. Monocytes were purified using the EasySep Mouse Monocyte Isolation Kit.

RNA sequencing. RNA sequencing was performed by the JP Sulzberger Columbia Genome Center. Poly-A pull-down was used to enrich mRNAs from total RNA samples (200 ng–1 μg per sample, RIN > 8 required). Libraries were prepared using the Illumina TruSeq RNA prep kit. Libraries were then sequenced using Illumina HiSeq2000. Multiplexed and pooled samples were sequenced to a depth of 24–34 × 10^6 reads per sample as 100-bp single-end reads. RTA (Illumina) was used for base calling, and bcl2fastq (version 1.8.4) was used for converting BCL to fastq format, coupled with adaptor trimming. Reads were mapped to a reference genome (mouse: UCSC/mm9) using Tophat (version 2.1.0) with 4 mismatches (–read-mismatches = 4) and 10 maximum multiple hits (–max-multihits = 10). To tackle the mapping issue of reads that are from exon–exon junctions, Tophat infers novel exon–exon junctions ab initio and combines them with junctions from known mRNA sequences (refgenes) as the reference annotation. The relative abundance (also known as the expression level) of genes and splice isoforms were estimated using cufflinks (version 2.0.2) with default settings.

ChIP–seq analysis. Track data of genes of interest were loaded into Galaxy[39] (http://usegalaxy.org) using the UCSC table browser and mouse mm10 genome. Using Galaxy, previously published ChIP–seq data[20–25] was then aligned to the mouse mm10 genome using the HISAT program (Galaxy version 2.03) with default settings. BamCoverage (Galaxy version 2.3.6.0) was then used to generate a coverage bigwig file, using default settings to scale to the size of the mm9 mouse genome. ComputeMatrix (Galaxy version 2.3.6.0) and plotHeatmap (Galaxy version 2.3.6.0) were then used to compare transcription factor occupancy at gene promoters, using the transcription start site as the reference point.

Dataset references. ChIP–seq data that were analysed were from the European Nucleotide Archive accession ERA319838 (IRF5), and from the following Gene Expression Omnibus accessions: GSE56123[20] (IRF1, IRF8, STAT1, STAT2); GSE67343[21] (IRF3); GSE36104[22] (IRF2, IRF4, NF-κB subunits); GSE62697[23] (IRF7); GSE77886[24] (IRF mutants); and GSE38379[25] (STAT1 knockout).

Patient sample selection and processing. We selected 10 consecutive patients, newly admitted to a medical or surgical intensive care unit (ICU), who had systemic inflammatory response syndrome and a known or suspected infection[40]. Patients were excluded from the study if they had an ICU admission or bacteraemia within the previous 30 days. After obtaining informed consent from the patient or a surrogate, whole blood was drawn within 4 h of ICU admission. Peripheral blood mononuclear cells were isolated from whole blood of healthy human volunteers or buffy coat isolates from patients from the ICU meeting sepsis criteria, by centrifugation on a Ficoll cushion. RNA was isolated with the miRNeasy micro kit (Qiagen 217084) and reverse transcribed as in 'RNA extraction, reverse transcription and qPCR'. Experiments were performed with approval of the Institutional Review Board at Columbia University and in accordance with regulations and guidelines set forth by the university. The results of these experiments are shown in Fig. 4a.

Patient sample selection and processing. Additional patient cohorts were obtained from hospitalized patients with acute decompensation of chronic liver disease and suspected bacterial infection. Baseline characteristics and outcome of patients with decompensated liver disease in the absence or presence of multiple organ failure syndrome (according to the EASL CLIF-C criteria for acute-on-chronic liver failure[41]) are given in Extended Data Fig. 8. Clinical scores—such as model for end-stage liver disease scores, bacterial culture count, protein analysis, blood count and serum levels of C-reactive protein and creatinine—were obtained from routine laboratory analysis. The determination of serum concentration of TNF was performed by ELISA. The results of these experiments are shown in Fig. 4b–f.

The isolation and characterization of human immune cells and the use of clinical data was approved by the internal review board (ethics committee of the Jena University Hospital, no. 3683-02/3). The study conformed to the ethical guidelines of the 1975 Declaration of Helsinki, and patients granted written informed consent before inclusion.

Statistics and sample collection. Student's *t*-tests were performed using the T.TEST function in Microsoft Excel. All other statistical tests were performed using Prism software. Unless otherwise stated, two-sided tests were performed. For samples using cell lines and cells isolated from inbred mice, the Student's *t*-test was often used. The distributional requirements for the test are assumptions. This means that—for instance—under the assumption of normal-distributed residuals, the *t*-test is an exact test. However, given a non-normal distribution of cell line data the test is not exact, but is instead approximative. For patient samples, nonparametric tests were used to avoid the assumption of a normal distribution. In all figures, error bars represent s.e.m. unless otherwise indicated. Standard deviations and s.e.m. values were calculated for each group of data and used to estimate variation (s.e.m. values are shown as error bars in most experiments). Variation generally appears similar between groups being compared. All experiments were replicated in the laboratory at least two times. Unless otherwise indicated, in experiments using primary cells *n* represents the number of experiments performed with separate cell isolations; in experiments using immortalized cells or cell lines, *n* represents the number of experiments performed using separate cell populations. Systematic randomization and blinding were not performed. Samples were excluded from the analysis if they were identified as outliers using the Grubbs' test (also known as the extreme studentized deviate method).

For mouse LPS-shock studies, an appropriate sample size was estimated on the basis of an outcome variable of survival time, measured in hours. An estimate was based on using a one-tailed Student's *t*-test to determine statistical significance. Control mice were expected to succumb within 62 h. Knockout mice were expected to become moribund 52 h after LPS injection at the latest. Therefore, the minimal effect size was estimated to be 10 h. On the basis of the literature and experiments previously performed by our laboratory, we anticipated a standard deviation of 10 h. Taking into account a power of 80% and alpha of 0.05, we calculated a sample size of 10 mice per genotype.

Reporting summary. Further information on experimental design is available in the Nature Research Reporting Summary linked to this paper.

Data accessibility. RNA sequencing data that support the findings of this study have been deposited in Gene Expression Omnibus (https://www.ncbi.nlm.nih.gov/geo/) with the accession code GSE89918. All other data are available from the corresponding author upon reasonable request.

35. Roberson, S. M. & Walker, W. S. Immortalization of cloned mouse splenic macrophages with a retrovirus containing the v-*raf/mil* and v-*myc* oncogenes. *Cell. Immunol.* **116**, 341–351 (1988).
36. Kertesz, M., Iovino, N., Unnerstall, U., Gaul, U. & Segal, E. The role of site accessibility in microRNA target recognition. *Nat. Genet.* **39**, 1278–1284 (2007).
37. Griffiths-Jones, S., Grocock, R. J., van Dongen, S., Bateman, A. & Enright, A. J. miRBase: microRNA sequences, targets and gene nomenclature. *Nucleic Acids Res.* **34**, D140–D144 (2006).
38. Ran, F. A. et al. Genome engineering using the CRISPR–Cas9 system. *Nat. Protocols* **8**, 2281–2308 (2013).
39. Afgan, E. et al. The Galaxy platform for accessible, reproducible and collaborative biomedical analyses: 2016 update. *Nucleic Acids Res.* **44**, W3–W10 (2016).
40. Bone, R. C. et al. Definitions for sepsis and organ failure and guidelines for the use of innovative therapies in sepsis. *Chest* **101**, 1644–1655 (1992).
41. Moreau, R. et al. Acute-on-chronic liver failure is a distinct syndrome that develops in patients with acute decompensation of cirrhosis. *Gastroenterology* **144**, 1426–1437.e9 (2013).
42. Rao, P. et al. IκBβ acts to inhibit and activate gene expression during the inflammatory response. *Nature* **466**, 1115–1119 (2010).

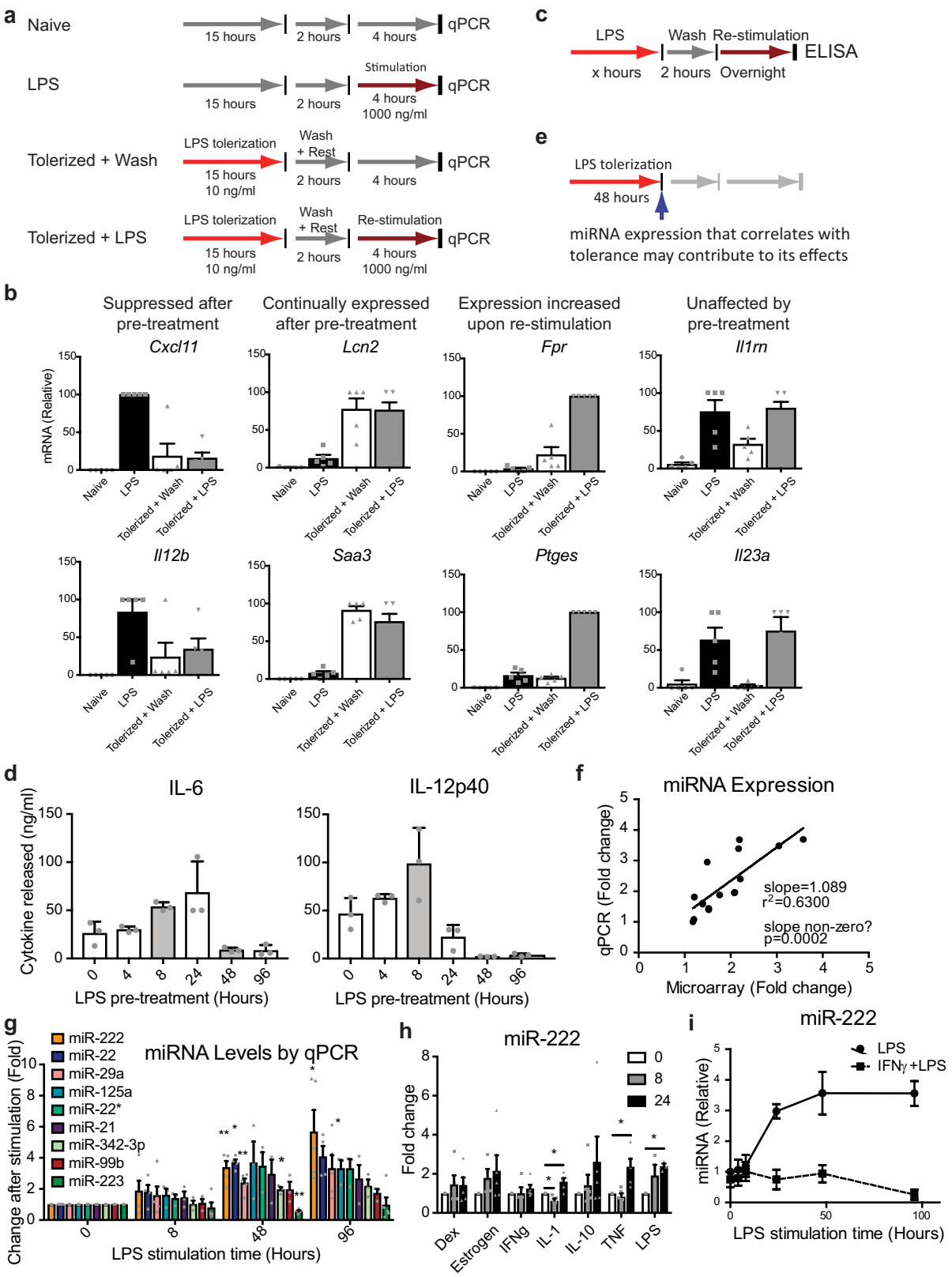

Extended Data Fig. 1 | See next page for caption.

Extended Data Fig. 1 | In vitro modelling of tolerance and miR-222 induction upon prolonged LPS stimulation. **a**, Schematic of experiments performed in **b**. **b**, Expression of LPS-response genes in control BMDMs that have undergone the given treatments. Four major expression patterns of LPS-response genes in response to tolerization were noted ($n = 5$ biologically independent samples). **c**, Schematic of experiments performed in **d**. **d**, Cytokine production—measured by ELISA—by BMDMs re-stimulated with LPS overnight after pre-treatment with LPS for the given periods of time. Time points chosen for miRNA microarray analysis have bars shaded in grey ($n = 3$ biologically independent samples). **e**, Schematic of strategy for experiments performed in Fig. 1. **f**, Comparison of microarray (x axis) and qPCR (y axis) measurements of LPS-induced upregulation of miRNAs. A linear regression showing the correlation between the two methods is plotted ($n = 16$ miRNAs tested). **g**, qPCR verification of LPS-induced change in expression of nine miRNAs ($n = 3$ biologically independent samples). **h**, Expression of miR-222 after stimulation of BMDMs by anti-inflammatory and tolerance-inducing factors for the given lengths of time ($n = 5$ biologically independent samples; Dex, dexamethasone). **i**, Expression of miR-222 in response to LPS alone, or LPS after pre-treatment of BMDMs with IFNγ ($n = 4$ biologically independent samples). For all bar and line graphs, mean ± s.e.m. is plotted. $^{*}P < 0.05$, $^{**}P < 0.01$, determined by two-sided Student's t-test for paired values.

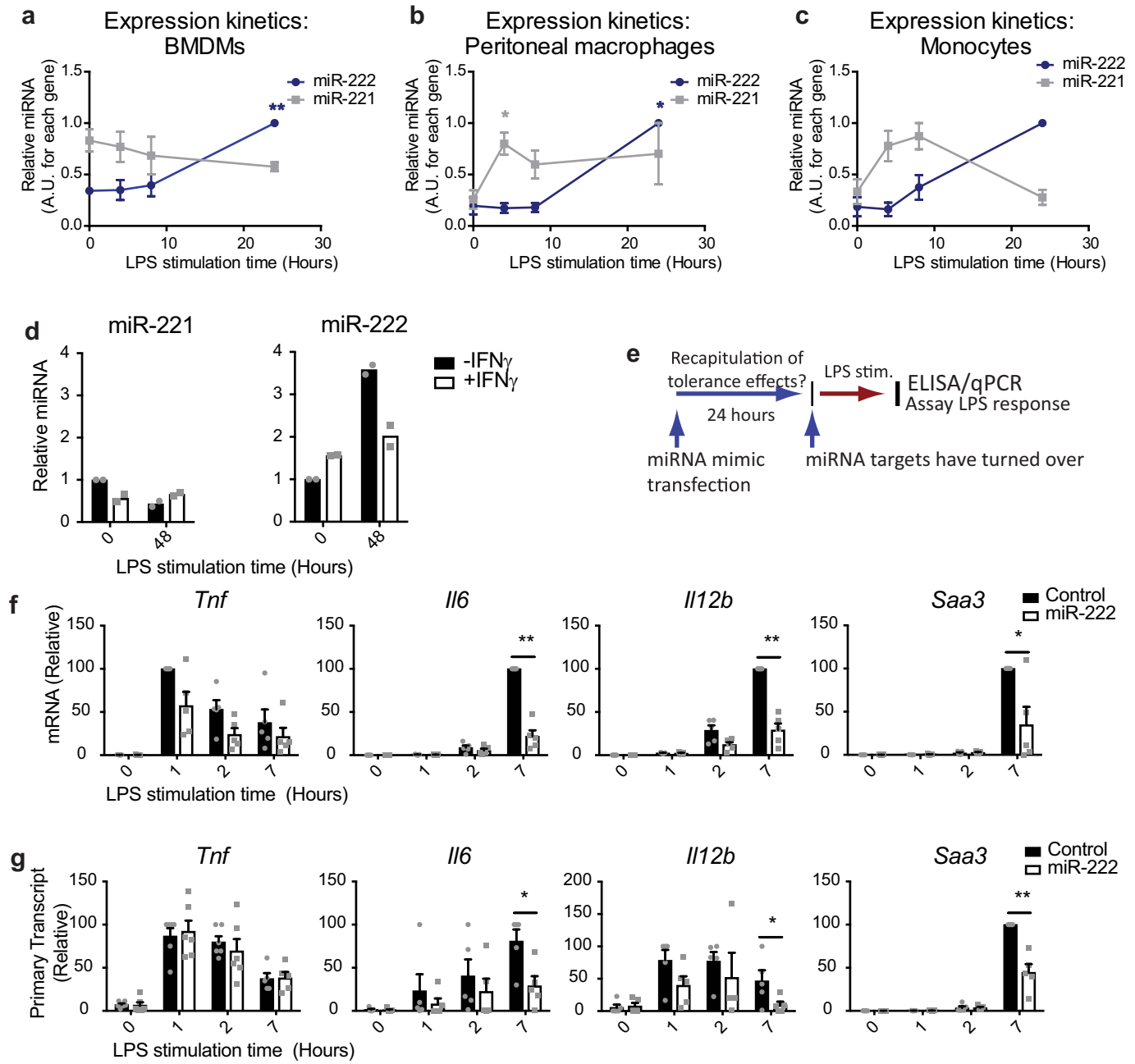

Extended Data Fig. 2 | Differential regulation of miR-222 and miR-221 and association of miR-222 with in vitro tolerance. a–c, Expression of miR-221 and miR-222 in response to LPS stimulation of BMDMs (**a**, $n = 4$ biologically independent samples), peritoneal macrophages (**b**, $n = 3$ biologically independent samples for miR-222 and $n = 4$ biologically independent samples for miR-221) or monocytes isolated from the bone marrow (**c**, $n = 3$ biologically independent samples), as determined by qPCR. **d**, LPS-induced miR-221 and miR-222 expression in BMDMs with or without IFNγ pre-treatment, as determined by qPCR ($n = 2$ biologically independent samples). **e**, Schematic of experiments performed in **f**, **g** and Fig. 1c. **f**, **g**, LPS-induced gene expression at the mRNA (**f**) or primary transcript (**g**) level after miR-222 mimic transfection ($n = 5$ biologically independent samples). For all bar and line graphs, mean ± s.e.m. is plotted. $^{*}P < 0.05$, $^{**}P < 0.01$, determined by two-sided Student's *t*-test for paired values.

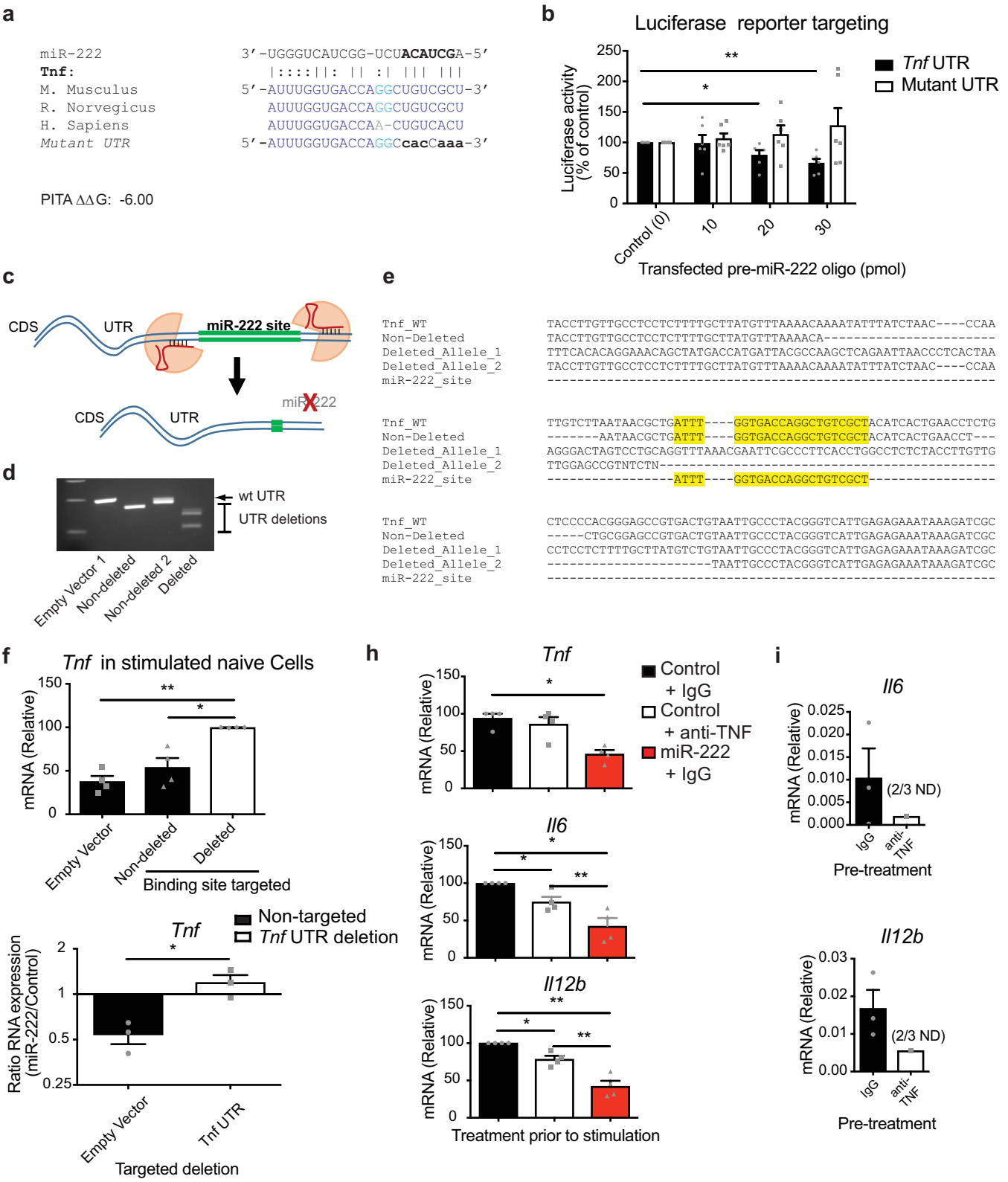

Extended Data Fig. 3 | See next page for caption.

Extended Data Fig. 3 | *Tnf* is a direct target of miR-222, but suppression of *Tnf* does not account for miR-222-mediated transcriptional silencing of late LPS-response genes. **a**, Sequence and prediction scores of an miR-222-binding site in the *Tnf* UTR. **b**, Activity of a luciferase reporter construct in which the luciferase coding sequence is followed by either the complete *Tnf* UTR, or a UTR in which the predicted miR-222-binding site has been mutated to the sequence shown in **a** ($n = 6$ independent experiments). **c**, CRISPR–Cas9 targeting strategy to delete predicted binding sites. CDS, coding sequence. **d**, Clones of RAW cells were screened for successful deletion of the miR-222-binding site by PCR across the targeted region of the UTR, using genomic DNA from the given clonal line as a template. Screening for *Tnf* UTR deletion is shown. Experiment was repeated twice with similar results. **e**, Successful deletion of the miR-222-binding site in RAW cell clones was confirmed by sequencing genomic DNA of the given cell line. miR-222-binding site in the *Tnf* UTR is highlighted in yellow. **f**, LPS-induced *Tnf* expression in control and CRISPR–Cas9-targeted RAW cells ($n = 4$ independent experiments). **g**, Average effect of miR-222 mimic transfection on LPS-induced *Tnf* mRNA levels in either control mouse embryonic fibroblasts or mouse embryonic fibroblasts that have undergone CRISPR targeting and clonal selection for deletion of the miR-222-binding site. Average of the effects from the three clonal lines ($n = 3$ independent experiments) is shown. **h**, Wild-type BMDMs were transfected with a control or miR-222 mimic oligonucleotide. Twenty-four hours later, cells were pre-treated with an isotype control (IgG) or TNF-neutralizing (anti-TNF) antibody for two hours, and stimulated with 10 ng ml^{-1} LPS. Expression of the given genes was measured by qPCR ($n = 4$ biologically independent samples). **i**, Efficacy of TNF neutralization was confirmed by treating cells with IgG or anti-TNF as above, followed by stimulation with 100 ng ml^{-1} recombinant mouse TNF ($n = 3$ biologically independent samples). Gene upregulation was not detected (ND) in two out of three samples treated with anti-TNF. For all bar graphs, mean ± s.e.m. is plotted. $^{*}P < 0.05$, $^{**}P < 0.01$, determined by two-sided Student's *t*-test for paired values.

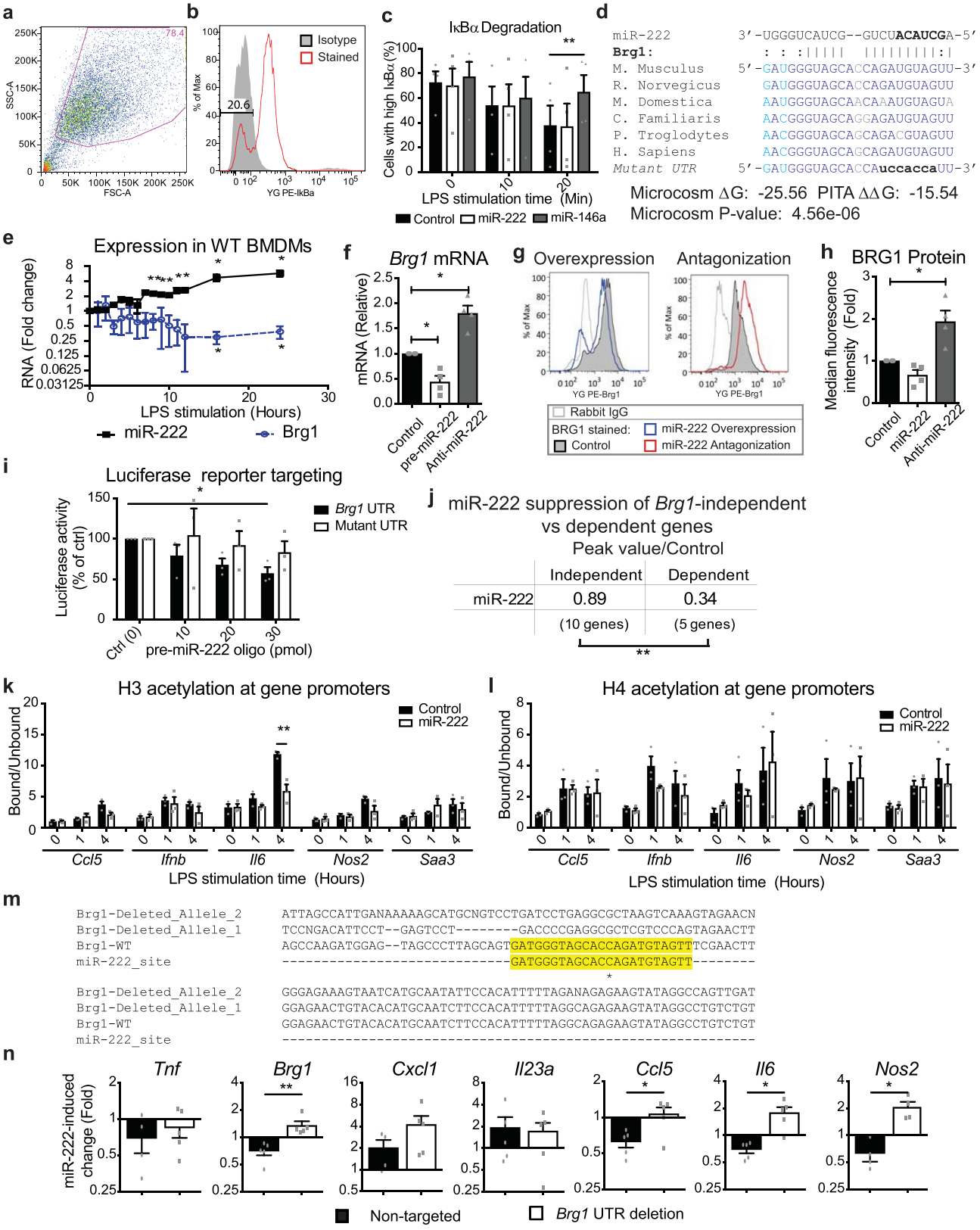

Extended Data Fig. 4 | See next page for caption.

Extended Data Fig. 4 | Evidence of miR-222 targeting of *Brg1*. **a**, Example of gating used to exclude dead cells from flow cytometry analyses in **c**, **g** and Extended Data Fig. 6i. **b**, Example of gating used to distinguish cells with high versus low levels of IκBα, as analysed in **c**. **c**, Effect of miRNA overexpression (by viral transduction) on LPS-induced IκBα degradation in immortalized BMDMs, measured by flow cytometry ($n = 4$ independent experiments). **d**, Sequence and prediction scores of an miR-222-binding site in the *Brg1* UTR. **e**, miR-222 and *Brg1* mRNA levels in LPS-stimulated BMDMs ($n = 3$ biologically independent samples). **f**, *Brg1* mRNA levels in resting BMDMs 24 h after transfection ($n = 4$ biologically independent samples). **g**, Effect of miRNA overexpression or antagonization (by viral transduction) on BRG1 levels in immortalized BMDMs, observed by flow cytometry. Representative of four independent experiments with similar results, quantified in **h**. **h**, Flow cytometry analysis of BRG1 protein levels in transduced immortalized BMDMs ($n = 4$ independent experiments). **i**, Activity of a luciferase reporter construct in which the luciferase coding sequence is followed by either the complete *Brg1* UTR, or a UTR in which the predicted miR-222-binding site has been mutated to the sequence shown in **d** ($n = 3$ independent experiments). **j**, Quantification of the average effect of miR-222 mimic transfection on *Brg1*-dependent and *Brg1*-independent LPS-response genes ($n = 3$ biologically independent samples). Two-sided Student's *t*-test for heteroscedastic values used to compare ratios (ratio of miR-222 overexpression to control) at peak LPS-induced expression times for *Brg1*-dependent versus *Brg1*-independent genes. **k**, **l**, ChIP for histone H3 acetylation (**k**) or histone H4 acetylation (**l**) after LPS stimulation of immortalized BMDMs transduced with overexpression constructs (**k** and **l** tested in same $n = 3$ independent experiments). **m**, Successful deletion of the miR-222-binding site in the *Brg1* UTR in RAW cell clones was confirmed by sequencing genomic DNA of the given cell line. miR-222-binding site is highlighted in yellow. **n**, Effect of miR-222 overexpression (by oligonucleotide transfection) on LPS-induced gene expression in either a RAW cell line in which the *Brg1*–miR-222 binding site was deleted by CRISPR targeting (as shown in Extended Data Fig. 3c) or a cell line in which the binding site was not targeted for deletion ($n = 5$ independent experiments). For all bar graphs, mean ± s.e.m. is plotted. $^{*}P < 0.05$, $^{**}P < 0.01$, determined by two-sided Student's *t*-test for paired values.

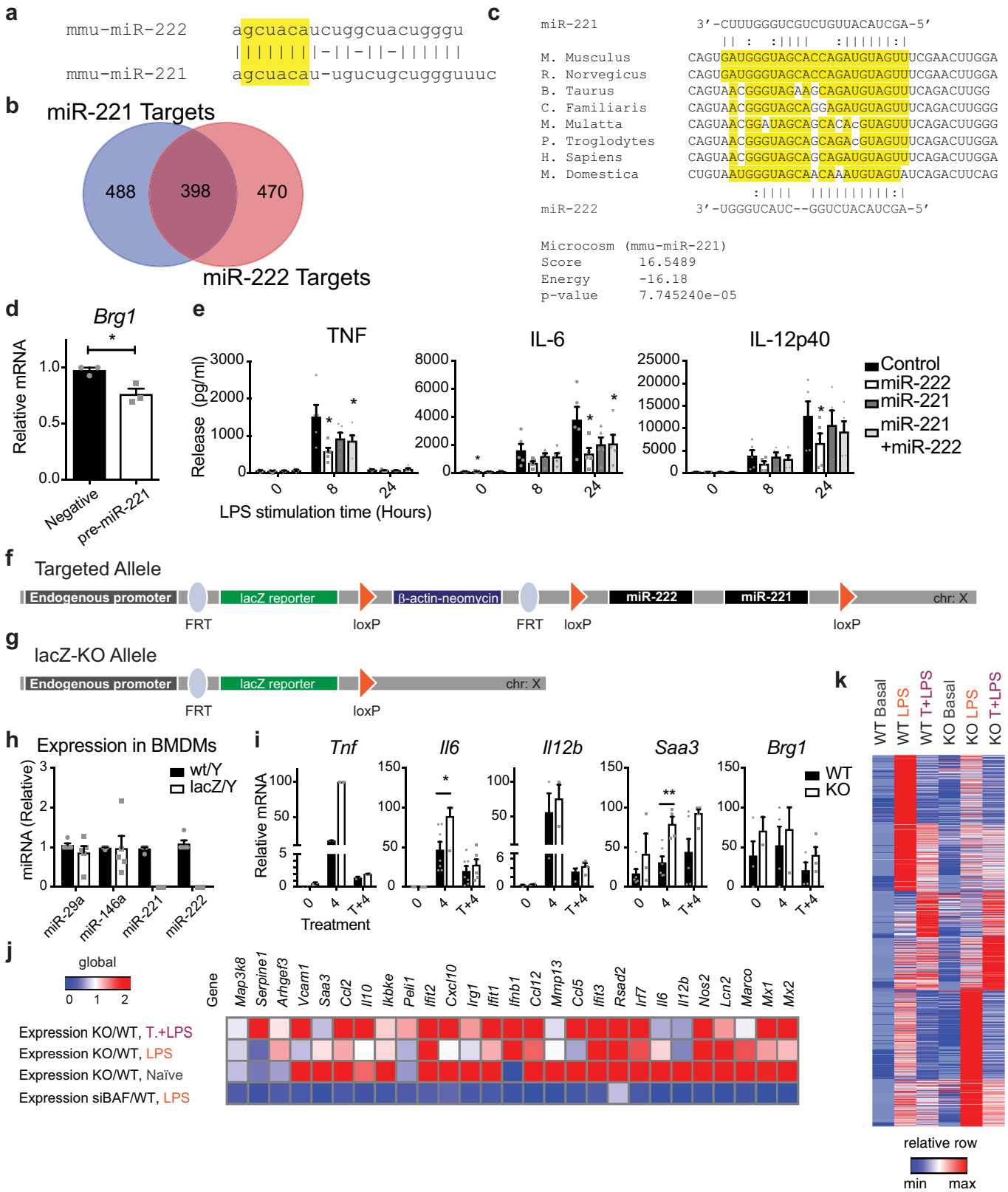

Extended Data Fig. 5 | See next page for caption.

Extended Data Fig. 5 | Comparison of miR-221 and miR-222, and effects of miR-221 and miR-222 deletion on the transcriptional response to LPS. a, Alignment of the mature miR-221 and miR-222 sequences. The miRNA seed sequence is highlighted in yellow. **b**, Venn diagram displaying overlap between MicroCosm target predictions for mmu-miR-221 and mmu-miR-222. **c**, Alignment and computational scores of miR-221 sequence with predicted *Brg1* UTR target site. Alignment of miR-222 sequence with the site is also shown. **d**, *Brg1* expression in BMDMs transfected with the given oligonucleotide ($n = 3$ biologically independent samples). **e**, LPS-induced cytokine production in BMDMs transfected with given miRNA mimics, as measured by ELISA ($n = 5$ biologically independent samples). **f**, Schematic of the miR-221 and miR-222 locus after targeting with a construct designed to generate both complete and conditional *mir-221 mir-222* knockout mice. **g**, Schematic of the miR-221 and miR-222 locus after breeding targeted mice (**f**) with EIIa-Cre mice, which results in complete deletion of miR-221 and miR-222. **h**, miRNA expression in BMDMs from littermates with a wild-type or *mir-221 mir-222* knockout allele ($n = 5$ biologically independent samples). **i**, LPS-induced gene expression in naive or tolerized peritoneal macrophages isolated from wild-type or *mir-221 mir-222* knockout littermates ($n = 7$ biologically independent samples). **j**, Heat map comparing the effect of *Brg1* and *Brm* knockdown[15] and *mir-222* knockout on gene expression. Colours represent values of the given ratios; red indicates increased expression, white indicates no change and blue indicates decreased expression. **k**, Heat map of LPS-induced gene expression in wild-type and *mir-221 mir-222* knockout macrophages. For all bar graphs, mean ± s.e.m. is plotted. $*P < 0.05$, $**P < 0.01$, determined by two-sided Student's *t*-test for paired (**d**, **e**) or heteroscedastic (**i**) values.

a **Genes higher basally in KO**

PANTHER GO-Slim Biological Process	Fold Enrichment	+/-	P value
response to interferon-gamma	10.63	+	1.66E-09
↳immune response	3.41	+	5.37E-08
↳immune system process	2.41	+	8.95E-03
cytokine-mediated signaling pathway	8.78	+	4.81E-24
localization	8.15	+	8.14E-13
locomotion	7.16	+	1.38E-13

Genes lower basally in KO

PANTHER GO-Slim Biological Process	Fold Enrichment	+/-	P value
macrophage activation	4.13	+	2.43E-02
cell-cell adhesion	2.98	+	1.98E-03
signal transduction	2.46	+	3.05E-03
Unclassified	.79	-	0.00E00

c **Genes higher in tolerized+LPS-stimulated KO**

PANTHER GO-Slim Biological Process	Fold Enrichment	+/-	P value
response to interferon-gamma	28.99	+	1.24E-07
↳immune response	5.54	+	1.34E-03
cytokine-mediated signaling pathway	17.81	+	3.24E-13
localization	12.46	+	4.41E-04
locomotion	9.43	+	2.68E-03

Genes lower in tolerized+LPS-stimulated KO

PANTHER GO-Slim Biological Process	Fold Enrichment	+/-	P value
behavior	32.35	+	2.80E-02
localization	22.14	+	7.92E-04
locomotion	16.76	+	3.02E-03
cytokine-mediated signaling pathway	16.63	+	3.99E-04

b **Genes higher in LPS-stimulated KO**

PANTHER GO-Slim Biological Process	Fold Enrichment	+/-	P value
response to interferon-gamma	15.14	+	5.61E-03
↳immune response	5.47	+	2.23E-04
cytokine-mediated signaling pathway	10.24	+	3.54E-06
macrophage activation	8.92	+	1.59E-02
cell-cell signaling	7.72	+	9.69E-03

Genes lower in LPS-stimulated KO

PANTHER GO-Slim Biological Process	Fold Enrichment	+/-	P value
Unclassified	.67	-	0.00E00

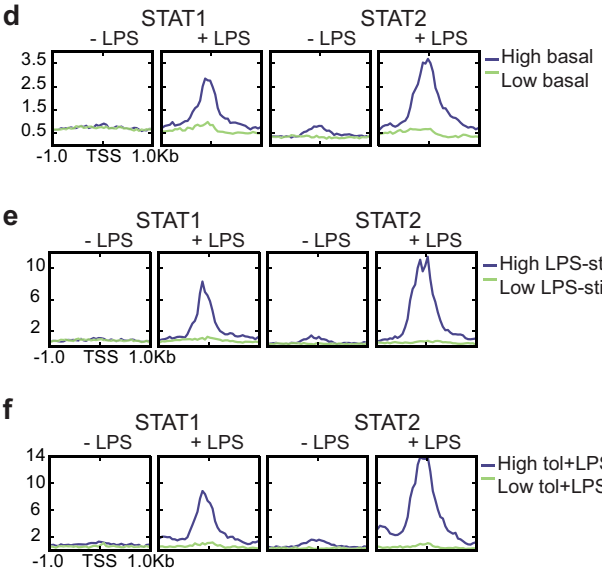

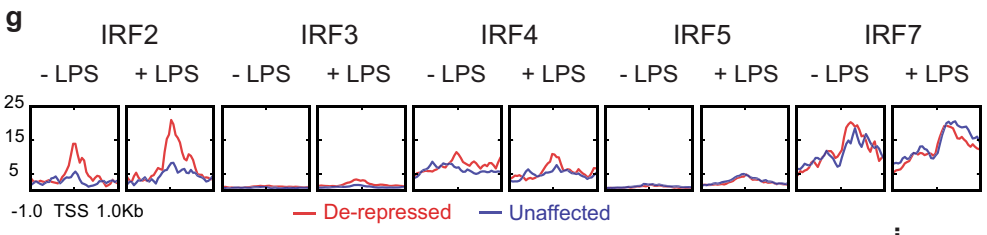

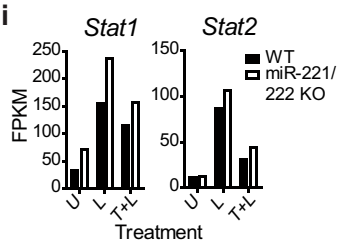

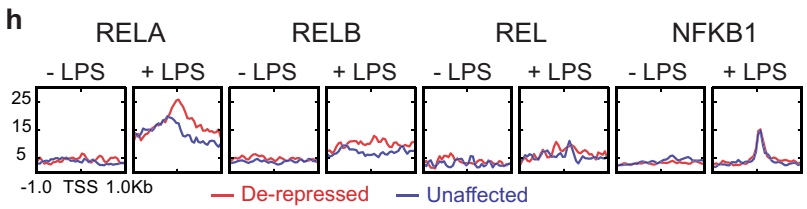

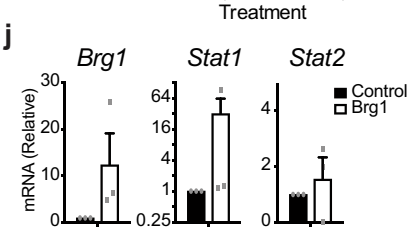

Extended Data Fig. 6 | Gene Ontology and ChIP–seq analysis shows that genes affected by *mir-221 mir-222* knockout have differential gene functions and transcription-factor binding at promoters. a–**f**, Enriched GO terms (**a**–**c**) and transcription-factor binding at promoters (**d**–**f**) of genes that are expressed at higher (twofold or higher) or lower (0.5-fold or lower) levels in *mir-221 mir-222* knockout macrophages after no stimulation (**a**, **d**, $n = 647$ genes higher, 565 genes lower), LPS stimulation (**b**, **e**, $n = 143$ genes higher, 121 genes lower) or LPS tolerization followed by re-stimulation (**c**, **f**, $n = 123$ genes higher,48 genes lower). PANTHER was used to identify GO terms. The top four terms for each category are shown; GO terms that are unique to either higher- or lower-expression gene subsets are highlighted. **g**, **h**, IRF and NF-κB subunit occupancy at gene promoters; gene subsets analysed are described in Fig. 2h. For transcription factor analyses, previously published ChIP–seq data were used[20–25]. **i**, RNA levels of genes in wild-type or *mir-221 mir-222* knockout peritoneal macrophages, quantified by a single RNA sequencing experiment. **j**, qPCR for gene expression in wild-type BMDMs after Amaxa-based nucleofection of given overexpression construct ($n = 3$ biologically independent samples). For all bar graphs, centre value represents the mean and errors bars (if applicable) represent s.e.m.

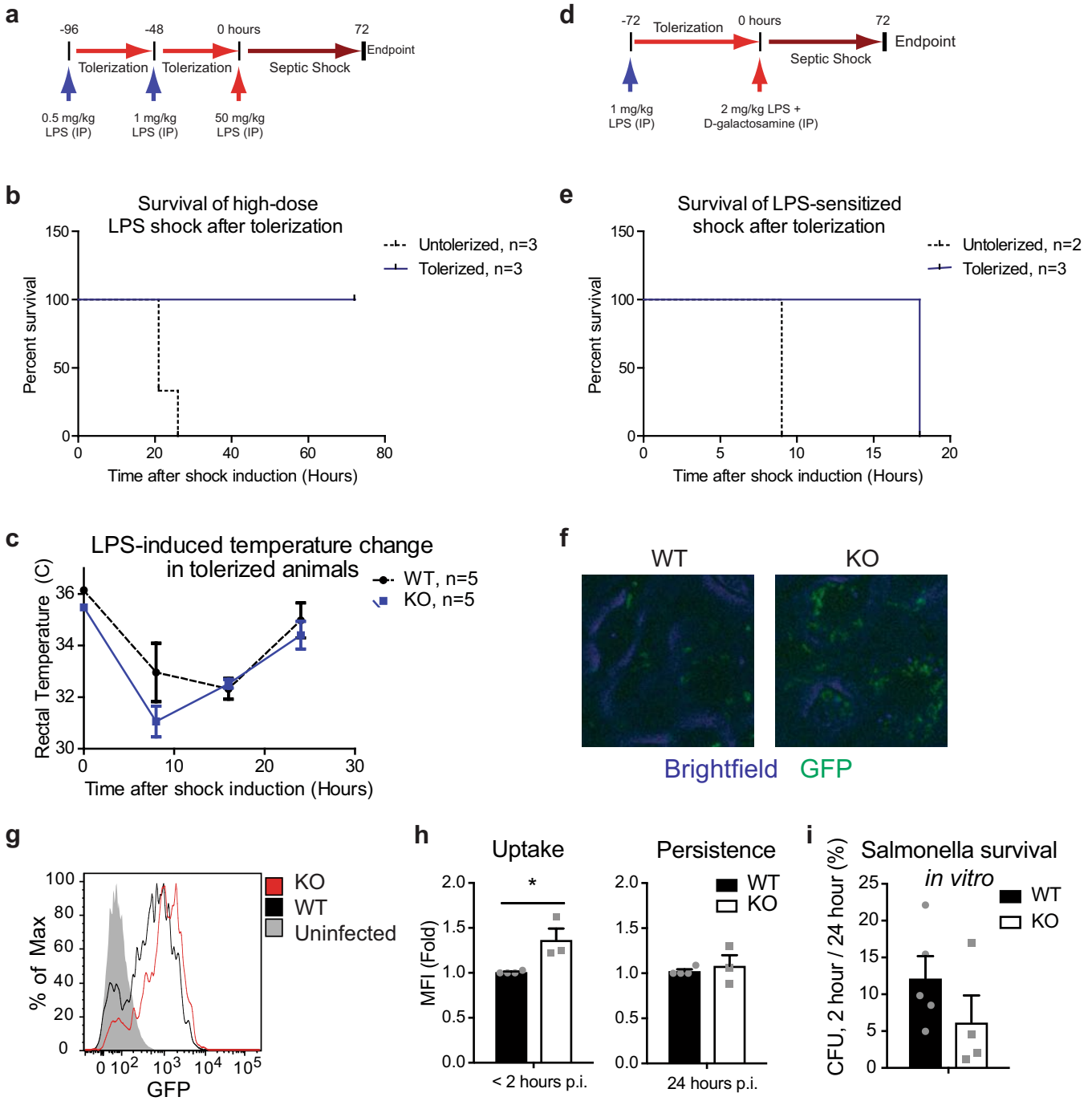

Extended Data Fig. 7 | *mir-221 mir-222* knockout mice have an altered LPS response and knockout macrophages exhibit enhanced *Salmonella* uptake and clearance in vitro. a, Schematic of experiments performed in **b**, **c**. **b**, Survival of naive or tolerized mice injected with high doses of LPS. **c**, Wild-type or *mir-222* knockout littermates were tolerized to LPS before lethal LPS injection. The change in body temperature after final LPS injection was monitored for 24 h. **d**, Schematic of experiments performed in **e**. **e**, Survival of naive or tolerized mice injected with LPS and D-galactosamine. **f**, BMDMs from wild-type or *mir-221 mir-222* knockout mice were spin-infected with a GFP-expressing strain of *S.* Typhimurium. Fluorescence was analysed by microscopy 60 min after infection. Representative of two independent experiments with similar results. **g**, BMDMs from wild-type or *mir-221 mir-222* knockout mice were spin-infected with a GFP-expressing strain of *S.* Typhimurium. Fluorescence was analysed by flow cytometry 30 min post-infection. Representative of three independent experiments with similar results. **h**, Average fluorescence of infected BMDMs after early (left) or late (right) time points after infection ($n = 4$ biologically independent wild-type samples, 3 biologically independent knockout samples). **i**, Survival of *S.* Typhimurium after in vitro infection of BMDMs, determined by comparing CFUs after lysis of BMDMs at early and late time points of infection ($n = 5$ biologically independent wild-type samples, 4 biologically independent knockout samples). For all bar and line graphs, mean ± s.e.m. is plotted. $^{*}P < 0.05$, $^{**}P < 0.01$, determined by two-sided Student's *t*-test for heteroscedastic values.

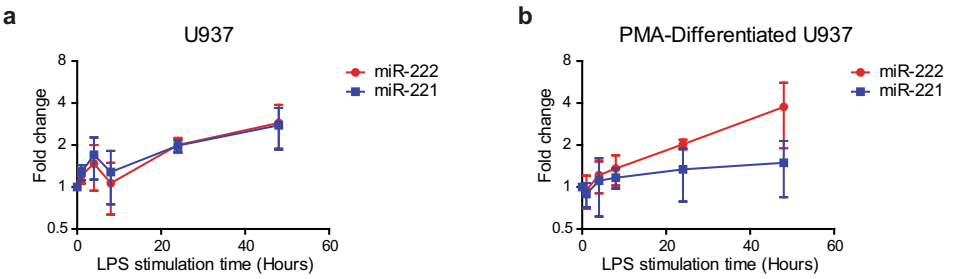

c

Characteristic	
Sex	
Male	6 (60%)
Female	4 (40%)
Age (years)	63 (53-74)
Operative reason for admission	
Yes	3 (30%)
No	7 (70%)
Mechanical ventilation	
Yes	5 (50%)
No	5 (50%)
White blood cell count (cells/mm3 x 1000)	12.9 (7.7-17.9)
Albumin (g/L)	2.5 (2.2-3.4)
Urine output (mL/24h)	895 (579-2463)
Pre-ICU length of stay (days)	1 (0-4)
APACHE IV score	62 (48-113)
SAPS II	48 (38-97)

d

	Acute Decompensation without organ failure N=16	Acute Decompensation with organ failure (ACLF) N=14	P value
Age (years)	58 (50-63)	64 (49-72)	0.29
Male sex	14 (88%)	11 (79%)	0.64
Alcoholic liver disease	11 (69%)	12 (86%)	0.40
ACLF grade (I/II/III)	0	9 (64%) / 3 (21%) / 2 (14%)	N/A
Bacterial infection			
- None	12 (75%)	8 (57%)	0.44*
- Peritonitis	2 (13%)	4 (29%)	
- Urinary tract	2 (13%)	1 (7%)	
- Pneumonia	0	1 (7%)	
Creatinine (µmol/l)	89 (75-108)	233 (186-299)	<0.001
Total bilirubin (µmol/l)	18 (11-47)	115 (25-310)	0.003
MELD score	10 (9-19)	29 (24-34)	<0.001
White blood cells ($x10^3$/µl)	6.9 (5.7-10.6)	9.3 (5.6-16.9)	0.28
C-reactive protein (mg/l)	18 (9-28)	25 (10-105)	0.19
Liver transplant or death within 30 days**	1 (6%)	6 (43%)	0.03

e

	Acute Decompensation without organ failure N=5	Acute Decompensation with organ failure (ACLF) N=5	P value
Age (years)	59 (53-70)	54 (46-59)	0.20
Male sex	5 (100%)	4 (80%)	1.00
Alcoholic liver disease	4 (80%)	5 (100%)	1.00
ACLF grade (I/II/III)	0	4 (80%) / 0 (0%) / 1 (20%)	N/A
Bacterial infection			
- None	5 (100%)	0	0.008*
- Peritonitis	0	5 (100%)	
- Urinary tract	0	0	
- Pneumonia	0	0	
Creatinine (µmol/l)	92 (52-110)	193 (123-367)	0.008
Total bilirubin (µmol/l)	16 (11-23)	57 (43-146)	0.008
MELD score	10 (9-11)	28 (21-36)	0.008
White blood cells ($x10^3$/µl)	7.2 (5.3-9.6)	13.6 (6.0-19.7)	0.22
C-reactive protein (mg/l)	33 (28-84)	76 (27-146)	0.75
Liver transplant or death within 30 days**	0	4 (80%)	0.048

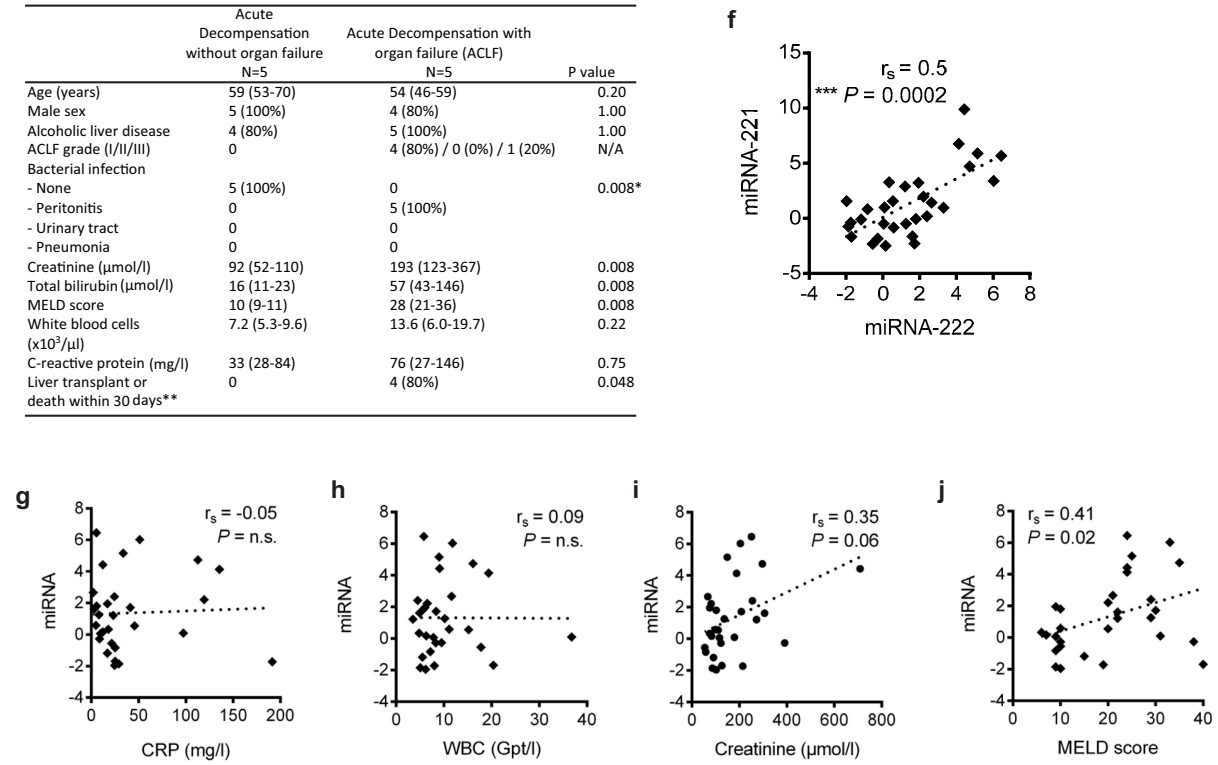

Extended Data Fig. 8 | See next page for caption.

Extended Data Fig. 8 | miR-221 and miR-222 are upregulated in human cells and patients with sepsis. a, **b**, LPS-induced miRNA expression in undifferentiated (**a**) or phorbol 12-myristate 13-acetate-differentiated (**b**) human U937 cells ($n = 3$ independent experiments). **c**, Patient characteristics for data shown in Fig. 4a. APACHE, acute physiology and chronic health evaluation; SAPS, simplified acute physiology score. Categorical variables are given as *n* (percentage in parentheses) and continuous variables as median (interquartile range in parentheses). **d**, **e**, Baseline characteristics of patients with decompensated liver disease in the absence or presence of multiple organ failure syndrome (according to the EASL CLIF-C criteria for acute-on-chronic liver failure). Data in **d** correspond to peripheral blood mononuclear cell analyses (Fig. 4b–d). Median with interquartiles or frequencies and percentages are shown. *P* values from Mann–Whitney *U* test or Fisher's exact test as appropriate (two-sided). *, comparing any infection to no infection; **, 4 out of 30 (13%) and 1 out of 10 (10%) patients were lost to follow-up within 30 days. Data in **e** correspond to monocyte analyses (Fig. 4f). Median with interquartiles or frequencies and percentages are shown. *P* values from Mann–Whitney *U* test or Fisher's exact test as appropriate (two-sided). *, comparing any infection to no infection; **, 1 out of 10 (10%) patients was lost to follow-up within 30 days. **f**, Correlation between miR-221 and miR-222 levels in patients characterized in **d** ($n = 30$ patients). Bivariate nonparametric correlation analysis (Spearman's rho) was used to identify correlations between variables and *P* values. **g**–**j**, Linear correlation of miR-222 expression and C-reactive protein (**g**), white blood cell count (**h**), creatinine levels (**i**) or model for end-stage liver disease score (**j**) in samples from the patient cohort described in **d** ($n = 30$ patients). Bivariate nonparametric correlation analysis (Spearman's rho) was used to identify correlations between variables and *P* values. For line graphs, mean ± s.e.m. is plotted.

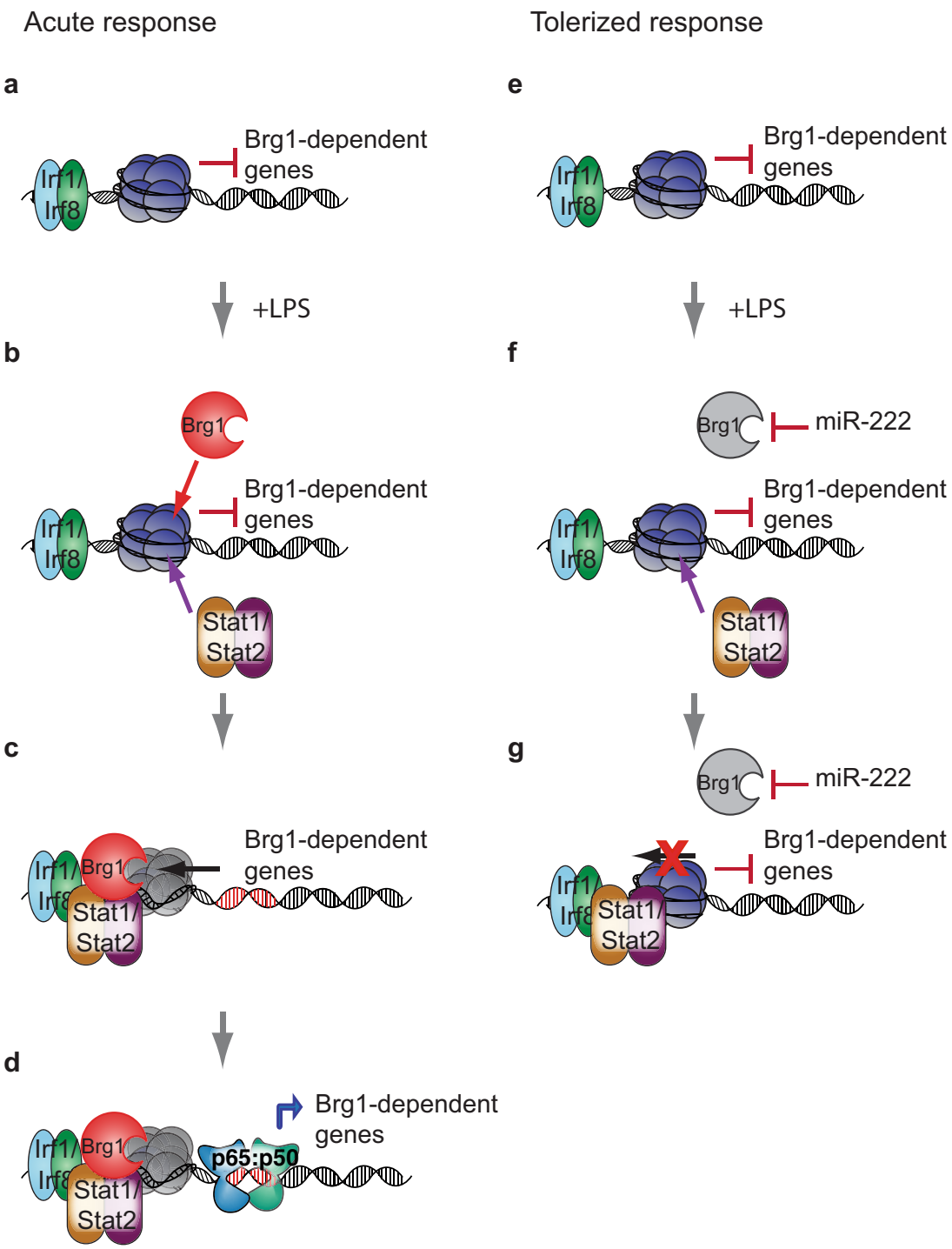

Extended Data Fig. 9 | Model of the effect of miR-222 on LPS-induced macrophage tolerance. a, Before an acute LPS stimulation, chromatin at BRG1-dependent gene promoters prevents binding of remodelling-dependent transcription factors and RNA polymerase. **b**, After an acute LPS stimulation, transcription factors such as STAT1 and STAT2 are recruited to gene promoters and stabilize BRG1 binding. **c**, **d**, BRG1 activity leads to chromatin remodelling (**c**), which enables recruitment of additional transcription factors, such as NF-κB, to the unwound DNA (**d**). This enables polymerase recruitment and licensing, which leads to gene transcription. **e**, After an initial LPS response, chromatin is 'reset' to an inhibitory state by negative regulators of chromatin accessibility. **f**, Upon LPS re-stimulation, transcription factors must again be recruited to gene promoters. However, miR-222 limits the level of BRG1. **g**, Lack of available BRG1 prevents chromatin remodelling at many gene promoters, and prevents downstream transcription factor recruitment. This prevents gene transcription from occurring in most cells.

Extended Data Table 1 | Identification of targets of miR-222

Predicted Target	Algorithm Score	P-Value	% Decrease
Mesdc1	16.1968	3.86E-09	31.83
Nfyb	16.5309	8.58E-07	31.90
Nfyb	16.027	8.58E-07	31.90
Sntb1	15.4316	2.95E-06	25.70
Smarca4	17.4905	4.57E-06	22.64
Dclre1a	15.2548	8.64E-06	22.67
Nudt5	16.5017	2.21E-05	82.49
Tpbg	16.3439	3.79E-05	75.81
Ptx3	15.9272	4.03E-05	50.04
Apaf1	15.3191	9.59E-05	39.79
Atp1a1	17.6386	9.74E-05	50.18
Pdhb	15.579	1.55E-04	26.18
Uchl1	15.4257	4.72E-04	20.26
Dhx9	16.4603	8.57E-04	96.82
Tsc2	20.1182	8.93E-04	40.97
Stmn1	16.5573	1.11E-03	82.55
Stmn1	16.009	1.11E-03	82.55
Ogfr	16.0031	1.13E-03	21.35
Ogfr	16.0031	1.13E-03	21.35
Ddx52	15.8837	1.30E-03	22.54
Zfp462	15.3834	1.55E-03	20.92
Sap30	17.1462	2.13E-03	37.05
Mad2l2	16.0031	2.22E-03	37.34
Idh2	15.8888	2.87E-03	47.13
Il19	17.0841	3.61E-03	53.02
Slc28a1	15.7179	4.02E-03	97.33
Tsc2	18.4316	4.61E-03	40.97
Capn7	15.7361	4.74E-03	24.89
Aldh2	15.5459	5.13E-03	23.55
Agpat2	18.2641	5.42E-03	40.86
Kcnh2	16.7713	5.47E-03	32.31
Cdca3	15.5835	5.53E-03	47.93
Plaur	15.7368	5.98E-03	57.51
Agpat2	18.1381	6.13E-03	40.86
Nfkbil1	17.832	6.74E-03	22.93
Slc23a3	17.9463	7.38E-03	96.59
Zyx	15.3325	7.52E-03	27.10
Nudt12	15.3316	7.53E-03	47.39
Nfkb1	15.676	7.54E-03	67.70
Nnt	15.7463	7.66E-03	30.32

(list continues on right)

Predicted Target	Algorithm Score	P-Value	% Decrease
Lcp1	16.0977	7.72E-03	45.12
Lrg1	15.3173	7.73E-03	22.69
Grip1	17.8508	8.09E-03	22.34
Golga1	15.2869	8.15E-03	28.15
Mapk6	15.3013	9.89E-03	36.07
Smarca4	17.4953	1.14E-02	22.64
Camp	15.6238	1.43E-02	39.31
Slc25a11	15.3352	1.46E-02	59.66
Sult1a1	15.2729	1.60E-02	31.32
4930544G11Rik	17.1192	1.64E-02	24.04
Cish	17.0804	1.70E-02	26.38
Pdcd10	15.3459	1.88E-02	63.49
Slc23a3	16.9058	2.01E-02	96.59
Qdpr	16.4511	2.06E-02	50.84
Pabpc1	16.86	2.10E-02	65.55
Cacnb2	16.0474	2.12E-02	34.44
Ddhd1	16.8345	2.15E-02	89.58
Dbnl	16.7678	2.29E-02	29.83
Ddhd1	16.696	2.45E-02	89.58
Rtn1	16.6889	2.47E-02	33.46
Exosc5	16.6889	2.47E-02	22.56
Fignl1	16.64	2.59E-02	23.59
2610020O08Rik	16.527	2.88E-02	21.06
Tnfsf11	16.4951	2.97E-02	22.56
Atox1	16.4786	3.02E-02	21.37
Fntb	16.3904	3.28E-02	26.90
4933402D24Rik	16.3904	3.28E-02	21.47
Olfr110	16.3782	3.32E-02	30.81
Mrpl3	15.4861	3.34E-02	63.03
Azi2	16.3295	3.47E-02	27.88
Tnks	16.326	3.48E-02	25.84
Fkbp9	15.872	3.58E-02	60.69
S100a4	16.2317	3.80E-02	78.00
Dtymk	16.2317	3.80E-02	20.44
Ppp1r14d	16.1174	3.82E-02	80.53
H47	16.2002	3.92E-02	24.67
Mrg2	16.1772	4.00E-02	32.25
Rpl27a	16.0727	4.41E-02	24.60
Impa2	16.0513	4.50E-02	66.38
Smarca4	16.0312	4.59E-02	22.64
Mad2l2	16.0031	4.71E-02	37.34
Cd33	15.9762	4.83E-02	46.63

miR-222 targets predicted by the MicroCosm program were filtered on the basis of their expression in macrophages. Only targets that decreased in expression after between 8 and 24 h of LPS stimulation (column 4) were considered (using microarray data generated in a previous study[42]). Results were then sorted by *P* value (generated by the MicroCosm program). *Brg1* is highlighted in red. Note that multiple listings for a target indicate that more than one site prediction for that gene was made by the MicroCosm program.

nature research

Corresponding author(s): Sankar Ghosh

Life Sciences Reporting Summary

Nature Research wishes to improve the reproducibility of the work that we publish. This form is intended for publication with all accepted life science papers and provides structure for consistency and transparency in reporting. Every life science submission will use this form; some list items might not apply to an individual manuscript, but all fields must be completed for clarity.

For further information on the points included in this form, see Reporting Life Sciences Research. For further information on Nature Research policies, including our data availability policy, see Authors & Referees and the Editorial Policy Checklist.

Please do not complete any field with "not applicable" or n/a. Refer to the help text for what text to use if an item is not relevant to your study.
For final submission: please carefully check your responses for accuracy; you will not be able to make changes later.

Experimental design

1. Sample size

Describe how sample size was determined.

For animal LPS shock studies, appropriate sample size was estimated based on an outcome variable of survival time, measured in hours. An estimate was based on using a one-tailed Student's t-test to determine statistical significance. Control animals were expected to succumb within 62 hours. Knockout animals were expected to become moribund 52 hours after LPS injection at the latest. Therefore, the minimal effect size was estimated to be 10 hours. Based on literature and experiments previously performed by our lab, we anticipated a standard deviation of 10 hours. Taking into account a power of 80% and alpha of 0.05, we calculated a sample size of 10 mice per genotype.

For other experiments, sample-size calculations were not performed. 3-5 initial experiments were performed; as this number of replicates was generally sufficient to confirm statistical significance of a result, further tests were not performed.

2. Data exclusions

Describe any data exclusions.

Samples were excluded from analyses if they were identified as outliers using the Grubbs' test, also called the ESD method (extreme studentized deviate).

3. Replication

Describe the measures taken to verify the reproducibility of the experimental findings.

All experiments were replicated in the laboratory at least 2 times on different days.
Whenever possible, biological replicates (as opposed to technical replicates) were used.
Thus, unless otherwise indicated, in experiments utilizing primary cells, n represents number of experiments performed with separate cell isolations; in experiments utilizing immortalized cells or cell lines, n represents the number of experiments performed using separate cell populations.

On occasion, replication attempts involving transfection of miRNA mimics or antagonists were not successful. We believe this to be the result of the poor transfection efficiency that is sometimes observed with macrophages.

For human participant data, patient cohorts from two different sites (Columbia University Medical Center and the Integrated Research and Treatment Center for Sepsis Control and Care) were tested. Samples were tested independently by researchers at each site.

4. Randomization

Describe how samples/organisms/participants were allocated into experimental groups.

Systematic randomization was not performed.
For BMDM studies, covariants were controlled by comparing the effects of different treatments on cells derived from the same animal.
For in vivo animal studies, covariants were controlled by performing tests on littermates.
For patient studies in Figure 4a, samples from sequential ICU patients admitted with the enrollment criteria were tested to limit potential biases in sample selection.

5. Blinding

Describe whether the investigators were blinded to group allocation during data collection and/or analysis.

Systematic blinding was not performed.
Blinding was not performed for BMDM/animal studies because the phenotypes being measured were expected to be readily quantifiable and not subjective in nature.
Blinding was not deemed necessary for the study of patient samples because no experimental intervention was performed.

Note: all in vivo studies must report how sample size was determined and whether blinding and randomization were used.

6. Statistical parameters

For all figures and tables that use statistical methods, confirm that the following items are present in relevant figure legends (or in the Methods section if additional space is needed).

n/a	Confirmed
☐	☒ The exact sample size (*n*) for each experimental group/condition, given as a discrete number and unit of measurement (animals, litters, cultures, etc.)
☐	☒ A description of how samples were collected, noting whether measurements were taken from distinct samples or whether the same sample was measured repeatedly
☐	☒ A statement indicating how many times each experiment was replicated
☐	☒ The statistical test(s) used and whether they are one- or two-sided *Only common tests should be described solely by name; describe more complex techniques in the Methods section.*
☐	☒ A description of any assumptions or corrections, such as an adjustment for multiple comparisons
☐	☒ Test values indicating whether an effect is present *Provide confidence intervals or give results of significance tests (e.g. P values) as exact values whenever appropriate and with effect sizes noted.*
☐	☒ A clear description of statistics including central tendency (e.g. median, mean) and variation (e.g. standard deviation, interquartile range)
☐	☒ Clearly defined error bars in all relevant figure captions (with explicit mention of central tendency and variation)

See the web collection on statistics for biologists for further resources and guidance.

Software

Policy information about availability of computer code

7. Software

Describe the software used to analyze the data in this study.

Microsoft Excel was used to perform two-sided t tests. GraphPad Prism software was used to generate all graphs and perform statistical analyses.
For microRNA targeting predictions, microCosm Targets version 5 (created on 07/07/2010 using the miRanda algorithm version 3.0) and PITA version 6 were used. All algorithm predictions were re-verified on December 5, 2013.
For flow cytometry analysis, Flowjo version 9 was used.
For RNA-seq analysis, bclfastq 1.8.4 with adaptor trimming, Tophat 2.1.0 (--read-mismatches=4 --max-multihits=10), and cufflinks 2.0.2 with default settings were used.
Gene ontology predictions were made using PANTHER version 11.1, released 10/24/2016.
ChIP-seq analysis was performed using the HISAT (Galaxy v. 2.03), BamCoverage (Galaxy v. 2.3.6.0), ComputeMatrix (Galaxy v. 2.3.6.0), and PlotHeatMap (Galaxy v. 2.3.6.0) programs.

For manuscripts utilizing custom algorithms or software that are central to the paper but not yet described in the published literature, software must be made available to editors and reviewers upon request. We strongly encourage code deposition in a community repository (e.g. GitHub). *Nature Methods* guidance for providing algorithms and software for publication provides further information on this topic.

Materials and reagents

Policy information about availability of materials

8. Materials availability

Indicate whether there are restrictions on availability of unique materials or if these materials are only available for distribution by a third party.

Unique materials will be made available from the authors or repositories.

9. Antibodies

Describe the antibodies used and how they were validated for use in the system under study (i.e. assay and species).

anti-IκBα (L35A5, Cell Signaling 4814) was recommended for detection of mouse IkBa by flow cytometry by the manufacturer.
anti-Brg1 (H88, Santa Cruz sc-10768) was recommended for detection of Brg-1 of mouse origin by WB, IP, IF and IHC(P) by manufacturer.
anti-Stat2 was a gift of Dr. Christian Schindler (Columbia University); specificity for mouse Stat2 ChIP was confirmed via use of knockout mouse cells (Fig. 2m)
The following control or secondary antibodies were used according to manufacturer specifications:
Rabbit mAb IgG Isotype Control (Cell Signaling 3900)
Alexa Fluor 488 Donkey Anti-Rabbit IgG (Invitrogen A21206)
Alexa Fluor 546 Goat Anti-Rabbit IgG (Invitrogen A11010)
Alexa Fluor 546 Donkey Anti-Mouse IgG (Invitrogen A10036)

10. Eukaryotic cell lines

a. State the source of each eukaryotic cell line used.

RAW 264.7 cells: ATCC TIB-7; 293FT cells: Invitrogen R7007; L-929 cells: ATCC CCL-1; U937 cells: ATCC CRL-1593.2

b. Describe the method of cell line authentication used.

Cells were purchased from vendor and tested for mycoplasma contamination prior to use (no further authentication of line identity was performed).

c. Report whether the cell lines were tested for mycoplasma contamination.

Cells tested negative for mycoplasma contamination after being received from vendor.

d. If any of the cell lines used are listed in the database of commonly misidentified cell lines maintained by ICLAC, provide a scientific rationale for their use.

No commonly misidentified cell lines were used.

Animals and human research participants

Policy information about studies involving animals; when reporting animal research, follow the ARRIVE guidelines

11. Description of research animals

Provide all relevant details on animals and/or animal-derived materials used in the study.

For BMDM generation, female mice 7-10 weeks of age were used, with the exception of Stat1/2 DKO BMDMs, for which male mice were used.
For in vivo experiments, male mice 6-10 weeks of age were used unless otherwise noted.
Experiments were performed with mice on the C57/Bl6 background.
miR-221/222 knockout mice were generated at the Columbia University Transgenic Mouse facility. miR-221/222 knockout mice were backcrossed to the C57Bl/6 background 5-8 times prior to experimental use.

Policy information about studies involving human research participants

12. Description of human research participants

Describe the covariate-relevant population characteristics of the human research participants.

Patient characteristics for data in Fig. 4a:
Characteristic
Sex
Male 6 (60%)
Female 4 (40%)
Age (years) 63 (53-74)
Operative reason for admission
Yes 3 (30%)
No 7 (70%)
Mechanical ventilation
Yes 5 (50%)
No 5 (50%)
White blood cell count (cells/mm3 x 1000) 12.9 (7.7-17.9)
Albumin (g/L) 2.5 (2.2-3.4)
Urine output (mL/24h) 895 (579-2463)
Pre-ICU length of stay (days) 1 (0-4)
APACHE IV score 62 (48-113)
SAPS II 48 (38-97)

Baseline characteristics of patients for Fig. 4b-d, followed by characteristics of patients for Fig. 4f:
Acute Decompensation without organ failure
N=16
Age (years) 58 (50-63)
Male sex 14 (88%)
Alcoholic liver disease 11 (69%)
ACLF grade (I/II/III) 0
Bacterial infection
- None
- Peritonitis
- Urinary tract
- Pneumonia
12 (75%)
2 (13%)
2 (13%)
0
Creatinine (µmol/l) 89 (75-108)
Total bilirubin (µmol/l) 18 (11-47)
MELD score 10 (9-19)
White blood cells (x103/µl) 6.9 (5.7-10.6)
C-reactive protein (mg/l) 18 (9-28)
Liver transplant or death within 30 days 1 (6%)

Acute Decompensation with organ failure (ACLF)
N=14
Age (years) 64 (49-72)
Male sex 11 (79%)
Alcoholic liver disease 12 (86%)
ACLF grade (I/II/III) 9 (64%) / 3 (21%) / 2 (14%)